Check for updates

Evolution of *Whirly1* in the angiosperms: sequence, splicing, and expression in a clade of early transitional mycoheterotrophic orchids

Rachel M. Muti[1,2], Craig F. Barrett[3] and Brandon T. Sinn[1,4]*

[1]Department of Biology and Earth Science, Otterbein University, Westerville, OH, United States, [2]Department of Hematology and Medical Oncology, Emory University, Atlanta, GA, United States, [3]Department of Biology, West Virginia University, Morgantown, WV, United States, [4]Faculty of Biology, University of Latvia, Riga, Latvia

The plastid-targeted transcription factor *Whirly1* (*WHY1*) has been implicated in chloroplast biogenesis, plastid genome stability, and fungal defense response, which together represent characteristics of interest for the study of autotrophic losses across the angiosperms. While gene loss in the plastid and nuclear genomes has been well studied in mycoheterotrophic plants, the evolution of the molecular mechanisms impacting genome stability is completely unknown. Here, we characterize the evolution of *WHY1* in four early transitional mycoheterotrophic orchid species in the genus *Corallorhiza* by synthesizing the results of phylogenetic, transcriptomic, and comparative genomic analyses with *WHY1* genomic sequences sampled from 21 orders of angiosperms. We found an increased number of non-canonical *WHY1* isoforms assembled from all but the greenest *Corallorhiza* species, including intron retention in some isoforms. Within *Corallorhiza*, phylotranscriptomic analyses revealed the presence of tissue-specific differential expression of *WHY1* in only the most photosynthetically capable species and a coincident increase in the number of non-canonical *WHY1* isoforms assembled from fully mycoheterotrophic species. Gene- and codon-level tests of *WHY1* selective regimes did not infer significant signal of either relaxed selection or episodic diversifying selection in *Corallorhiza* but did so for relaxed selection in the late-stage full mycoheterotrophic orchids *Epipogium aphyllum* and *Gastrodia elata*. Additionally, nucleotide substitutions that most likely impact the function of *WHY1*, such as nonsense mutations, were only observed in late-stage mycoheterotrophs. We propose that our findings suggest that splicing and expression changes may precede the selective shifts we inferred for late-stage mycoheterotrophic species, which therefore does not support a primary role for *WHY1* in the transition to mycoheterotrophy in the Orchidaceae. Taken together, this study provides the most comprehensive view of *WHY1* evolution across the angiosperms to date.

KEYWORDS

mycoheterotrophy, *Corallorhiza*, orchid, genomic stability, intron retention, transcription factor, plastome evolution, *Whirly1*

1 Introduction

The ability to photosynthesize has been lost dozens of times across the angiosperm Tree of Life, and at least 30 independent losses have occurred in the Orchidaceae (Merckx and Freudenstein, 2010; Barrett et al., 2014, Barrett et al, 2019). Mycoheterotrophy, the derivation of carbon nutrition from fungi (Leake, 1994), is common to all orchids during early development and is a nutritional requirement due to the lack of endosperm in their seeds (Rasmussen, 1995, Rasmussen, 2002). In lieu of stored nutrition, orchid seeds have evolved a complex symbiotic relationship with fungi, where orchid seeds germinate only in the presence of an appropriate fungal partner and the nutrition required for embryo development is derived exclusively via the degradation of fungal hyphae which penetrate the orchid cells (Merckx and Merckx, 2013; Zeng et al., 2017; Yuan et al., 2018). The duration of reliance upon their fungal partner for nutrition has been extended in some orchid species, which have evolved to parasitize fungi for the entirety of their lives. Independent shifts to a mycoheterotrophic condition throughout the angiosperms have independently led to plastid genome (plastome) degradation (Barrett et al., 2014; Wicke et al., 2016; Graham et al., 2017; Timilsena et al., 2023), elevated rates of nucleotide substitution (Lemaire et al., 2010; Wicke et al., 2016), and oftentimes the loss of morphological structures such as leaves and roots (Leake, 1994).

Corallorhiza is a North American, temperate genus comprising 12 species of morphologically reduced, mycoheterotrophic orchids for which varying states of plastome degradation and inferred photosynthetic ability have been characterized (Barrett and Freudenstein, 2008; Zimmer et al., 2008; Cameron et al., 2009; Barrett and Davis, 2012; Barrett et al., 2014, Barrett et al, 2018). The presence of relatively intact plastomes containing the expected repertoire of housekeeping genes in *Corallorhiza* species evidences the clade as a group of early transitional mycoheterotrophs, in contrast with late-stage mycoheterotrophic species which have highly degraded plastomes and lack many or all plastid housekeeping genes, such as *Epipogium* and *Gastrodia* species (*sensu* Barrett and Davis, 2012; see also Barrett et al., 2014). *Corallorhiza* species parasitize Basidiomycete fungi that are engaged in mycorrhizal relationships with nearby autotrophic plants, predominantly in the families Russulaceae and Thelephoraceae (Taylor and Bruns, 1997; Barrett et al., 2010; Freudenstein and Barrett, 2014; Taylor et al., 2022). In addition to their relationship with fungi, a conspicuous characteristic of *Corallorhiza* species is the complete loss of both leaf laminae and roots. A recurrent theme of morphological reduction has been documented across parasitic and mycoheterotrophic plant lineages (see Leake, 1994), and work has recently focused on genomic content and gene expression in mycoheterotrophic species in order to improve our understanding of the genomic precursors and consequences of this trophic transition (Barrett et al., 2014; Wicke et al., 2016; Graham et al., 2017; Zhang et al., 2017; Yuan et al., 2018; Cai, 2023; Timilsena et al., 2023).

The integrity of the plastome of parasitic and mycoheterotrophic plants is of particular interest as reduction in gene content, increased number of pseudogenes, structural variation, and a reduction in overall genome length have been found to correlate with the degree of external carbon reliance among parasitic angiosperms. Generally, disruptions to the genome such as double-strand DNA breaks are harmful to the organism, and many mechanisms that help to protect against such occurrences have evolved throughout the Tree of Life (Waterworth et al., 2011). One such genome stabilizing mechanism that is increasingly recognized for its involvement in processes such as plastome double-strand break repair is the activity of the Whirly family of transcription factors (*WHY*; Desveaux et al., 2005).

Transcription factors are regulatory gene products that function by binding to DNA (Latchman, 1993). The Whirly family comprises *WHY1*, *WHY2*, and *WHY3*, which are three plant-specific, nuclear-encoded genes with DNA-binding domains, that are named for their whirligig-like structural conformation (Desveaux et al., 2002; Cappadocia et al., 2010). Crystal structures of the Whirly transcription factors have been determined as tetramers that have a single-stranded DNA-binding domain that spans two subunits (Cappadocia et al., 2013). Of particular interest is *WHY1*, the product of which has been implicated to play roles in several processes including mediation of abiotic stressors (Zhuang et al., 2019, Zhuang et al, 2020; Ruan et al., 2022), induction of double-strand DNA break repair (Cappadocia et al., 2010), and plastid biogenesis (Prikryl et al., 2008). Transcription factors (TF) are crucial to many regulatory and developmental processes, which is reflected in the massive expansions of many TF gene families in plants (Lehti-Shiu et al., 2017). Our present understanding of TF evolution has largely been informed through the investigations focused on understanding their roles in morphological or ecological diversification (see de Mendoza et al., 2013; Lai et al., 2020) rather than how they change in systems, which have undergone coincident extreme loss of morphological and genomic features.

WHY1 has been shown to dually localize to both plastids and the nucleus (Krause et al., 2005; Grabowski et al., 2008; Prikryl et al., 2008; Isemer et al., 2012; Ren et al., 2017). In chloroplasts, *WHY1* localizes to the boundary between the thylakoid and nucleoid membrane in chloroplasts and has been implicated in retrograde signaling regulating H_2O_2 homeostasis and as a coordinator of photosynthetic gene expression (Lepage et al., 2013; Foyer et al., 2014; Lin et al., 2019). Species that have undergone the transition to heterotrophy experience elevated levels of oxidative stress compared to autotrophic relatives (Suetsugu et al., 2017; Lallemand et al., 2019). Additionally, *WHY1* proteins stabilize plastid genomes by non-specific binding to the genome, which protects against microhomology-mediated DNA rearrangements, including deletions and duplications of sequences (Maréchal et al., 2009; Lepage et al., 2013; Zampini et al., 2015).

WHY1 is involved in complex roles in both plant defense responses and genomic stabilization. For example, mutations which reduce the binding affinity of *WHY1* correlate with increased infection by some pathogens (Desveaux et al., 2004). *WHY1* has been shown to bind to specific DNA promoter regions that can induce transcription (Zhuang et al., 2020), aid in defense response signaling and accumulation of disease resistance (Desveaux et al., 2004, Desveaux et al, 2005), and also maintain telomere length in the nuclear genome (Desveaux et al., 2005).

Recently, *WHY1* has even been shown to be capable of negatively regulating the RNA interference response to two geminiviruses (Sun et al., 2023). Taken together, the literature suggests that modulation of *WHY1* expression can result in tradeoffs between plant defense and genomic stability.

The roles that *WHY1* plays in stabilizing both the nuclear and plastid genomes (Yoo et al., 2007; Zampini et al., 2015), defense response (Desveaux et al., 2005), and chloroplast development (Qiu et al., 2022) are central to our choice to study the evolution of this transcription factor. In particular, experimental work demonstrating plastome destabilization (Lepage et al., 2013; Zampini et al., 2015), albinism, and variegation in *WHY1* mutants (Prikryl et al., 2008; Ren et al., 2017; Qiu et al., 2022) makes the gene a compelling target given the reduction in plastome content and length observed across parasitic angiosperms (Barrett et al., 2014; Wicke et al., 2016). To date, work characterizing the sequence and expression diversity of *WHY1* has been restricted to model or agricultural systems (Cappadocia et al., 2013; Ruan et al., 2022; Taylor et al., 2022) and no phylo-comparative investigations of sequence evolution and selective regime have been conducted. The implication of *WHY1* in processes associated with the mycoheterotrophic condition frames a phylogenetically informed investigation of *WHY1* along a trophic gradient as an important step in improving our understanding of the evolution of plastid-targeted TFs in heterotrophic plant lineages.

We focus on four species, *C. trifida*, *C. striata*, *C. wisteriana*, and *C. maculata*, which together comprise an early transitional trophic gradient to full mycoheterotrophy with sister relationships among partial and full mycoheterotrophs (Figure 1). The well-characterized phylogenetic relationships between these four *Corallorhiza* species (Barrett et al., 2018) provide a powerful framework upon which to investigate *WHY1* evolution during the early stages of transition to full mycoheterotrophy while accounting for phylogenetic non-independence (*sensu* Felsenstein, 1985). We consider *C. trifida* and *C. wisteriana* to be partial mycoheterotrophs, as their tissues contain measurable chlorophyll content and their plastomes are the most genetically intact plastid genomes in the genus, although photosynthesis has only been directly observed in *C. trifida* (Zimmer et al., 2008; Cameron et al., 2009; Barrett et al., 2014, Barrett et al, 2018). Conversely, we consider *C. maculata* and *C. striata* to be fully mycoheterotrophic, evidenced by their highly reduced chlorophyll content and degradation of many photosynthesis-related genes (Barrett et al., 2014, Barrett et al, 2018).

Here, we characterize the evolution of *WHY1* across a mycoheterotrophic gradient, framed by phylogenetic context provided by the broadest taxonomic sampling of the gene to date, including late-stage mycoheterotrophic orchid species from the genera *Epipogium* and *Gastrodia*. Our integrative work leverages a combination of novel and publicly available data generated from DNA sequencing, RNA sequencing (RNA-seq), and Oxford Nanopore sequencing from 110 angiosperm species representing 21 orders. Taken together, the results of our analyses of *WHY1* sequence, expression, splicing, and selective regime across both a trophic gradient and the angiosperms more broadly suggest that the gene may play a critical role in maintaining plastome stability after the transition to mycoheterotrophy.

2 Materials and methods

2.1 Publicly available sequences

Annotated *WHY1* sequences were obtained from the nucleotide and Ref-seq National Center for Biotechnology Information (NCBI) databases and Orchidstra, an orchid-specific database (Chao et al., 2017). Only *WHY1* sequences containing canonical *WHY1* ORFs (open reading frames) were retained. Additionally, sequences were excluded if they did not contain the ssDNA-binding region (KGKAAL; *A. thaliana* Q9M9S3) as reported by Cappadocia et al. (2013; PDB 4KOO). Identical sequences were excluded for taxa with multiple database accessions. Stop codons were trimmed from sequences, with the exception of premature stop codons in sequences from known mycoheterotrophs, which were changed to gap characters (-) for compatibility with downstream methods (e.g., HyPhy, see below). In total, 110 species were included in the angiosperm-wide alignment (see Alignment section below; Supplementary Table S1).

2.2 RNA-seq, *de-novo* assembly of transcripts, and *in-silico* differential expression

Corallorhiza tissues used for RNA-seq are those referred to in Sinn and Barrett (2020), where complete methodological details can be found. In brief, total RNAs were extracted from pooled tissues using the ZR Plant RNA MiniPrep Kit (Zymo Research, Irvine, California, USA), leveraging a DNA exclusion column and a DNase digestion step. RNA extractions were conducted in an area where both DNA and RNase contamination were actively managed, the later with both RNase Away and RNase Zap (Thermo Fisher Scientific, Waltham, Massachusetts, USA). Pooled tissues were categorized as either aboveground (combined stem, flower, and ovary tissues) or belowground (rhizome tissue, including fungal tissue), and three biological replicates of each tissue type were extracted for all four species. Extracted RNAs were quantified on a 2100 Bioanalyzer (Agilent, Santa Clara, California, USA) and a NanoDrop spectrophotometer (Thermo Fisher Scientific, Waltham, Massachusetts, USA). Library construction was conducted at the West Virginia University Genomics Core Facility using TruSeq Stranded mRNA kit (Illumina, San Diego, California, USA). Libraries were sequenced on the Illumina HiSeq 1500 platform at the Marshall University Genomics Core Facility, with the exception of aboveground *C. maculata* (two samples) and belowground *C. striata* (two samples) for which library preparation of limited material was not successful.

De-novo assembly of transcripts from each *Corallorhiza* species was conducted using Trinity (version v2.13.2, Grabherr et al., 2011). Reads were trimmed using Trimmomatic (version 0.36, Bolger et al., 2014) with default settings to remove sequencing adapters and low-quality bases from the read ends. Trinity was provided with a samples file with biological replicate relationships, and strand-specific (SS) library type was set to reverse-forward (RF). Trimmed

reads were mapped to each assembled transcript using the splice-aware read mapper BBMAP (version 38.96; Bushnell, 2022) with default settings, with mapped reads output to SAM format and converted to sorted BAM-formatted files using SAMtools (version 1.15; Li et al., 2009).

In-silico analysis of differential expression was conducted using scripts provided as components of the Trinity RNA-seq pipeline (Haas et al., 2013). Transcript abundance was estimated using the alignment-free estimation method as implemented in Salmon (version 1.2.0, Patro et al., 2017). The strand-specific library type was set to RF. Salmon output files included transcript abundance estimates at both the transcript and gene level. Matrices were built using the abundance_estimates_to_matrix.pl script for both transcript counts and gene expression. Differential expression analysis was run using the R (R Core Team, 2019) package edgeR (Bioconductor version 3.10, Robinson et al., 2010) via the run_DE_analysis.pl script, which identified differential expression using biological replicates of tissues across the replicate conditions aboveground and belowground. TPM (transcripts per million) values were normalized using the TMM (trimmed mean of M-values; Robinson and Oshlack, 2010) approach in order to normalize expression values while maintaining comparability of expression between samples.

2.3 Identification of *WHY1* transcripts

We used the HMMER suite (version 3.3.2; Eddy, 2011) to create a *WHY1* hidden Markov model (HMM) profile. The HMM profile was built with hmmbuild, which used the complete angiosperm-wide *WHY1* nucleotide alignment. All assembled *Corallorhiza* transcripts were then searched against the HMM model using nhmmer (Wheeler and Eddy, 2013). Default parameters were used for both programs. All assembled isoforms of a transcript identified with the highest *E*-value were considered as potential splicing variants of *WHY1*.
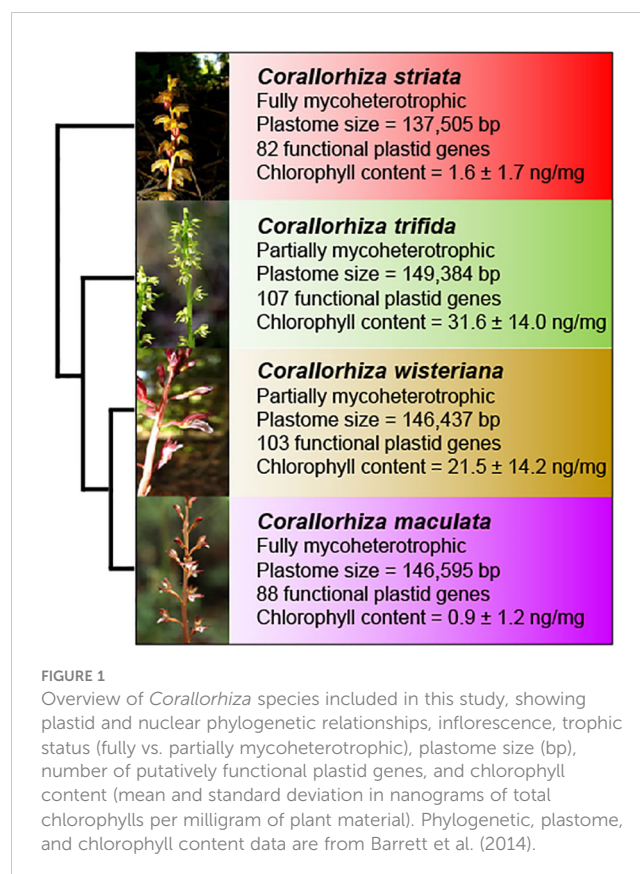
2.4 PCR amplification

Primers for amplification of genomic *WHY1* sequence were designed using the Geneious Prime (version 2020.2.4, https://www.geneious.com) plugin for Primer3 (version 2.3.7; Untergasser et al., 2012). Oligos were synthesized by Integrated DNA Technologies (Coralville, Iowa, USA). Genomic sequences presented here were amplified using a forward primer (WHY1_upstreamF: TTC AAA TCG AAG AGT AAA CTA ACC) whose 3' end binds five nucleotides upstream of exon 1 and a reverse primer (WHY1_exon2R: TTT GGC TCA ACT GAT AGA GC), which binds in the downstream portion of exon 2. PCR amplification of *WHY1* for each *Corallorhiza* species was performed on CTAB extractions (Doyle and Doyle, 1987) of total DNA. PCR was conducted in 25 µl volumes, comprising 12.5 µl of Apex Taq RED Master Mix (Genesee Scientific; Morrisville, North Carolina, USA), 1.25 µl of each forward and reverse primer, 9 µl of water, and 1 µl of template DNA. PCR was conducted in a Bio-Rad T100 Thermocycler (Hercules, California, USA) using the following

program: initial template denaturation at 95°C for 3 min, followed by 30 cycles of denaturation at 95°C for 30 s, primer annealing at 52°C for 30 s, and template extension at 72°C for 30 s. The program ended with a final extension at 72°C for 5 min and was held at 4°C until retrieval. PCR cleanup was performed with Agencourt AMPure XP PCR Purification beads (Beckman Coulter Life Sciences; Indianapolis, Indiana, USA). Purified DNA samples were quantified using a NanoDrop One[C] spectrophotometer (Thermo Fisher Scientific) and a Qubit fluorometer (Thermo Fisher Scientific) with the dsDNA BR Assay Kit.

2.5 Nanopore sequencing

Purified DNA samples were diluted to equimolar concentrations and libraries for long-read sequencing were prepared according to the Oxford Nanopore Technologies (ONT; Oxford, United Kingdom) End-Prep protocol (SQK-LSK109). The library of each *Corallorhiza* species received a unique barcode for Nanopore sequencing using the Native Barcoding Expansion 1–12, PCR-free kit (EXP-NBD104). The MinION SpotON flow cell (R9.4.1 FLO-MIN 106; ONT) was used for sequencing. Base calling was performed using the high-accuracy base calling algorithm as implemented in the GPU version of Guppy (version 6.2.1 + 6588110a6; ONT) on an NVIDIA GeForce RTX 2060 graphics card. Nanopore reads were mapped to the *Dendrobium catenatum* (RefSeq ID: GCF_001605985.2; Zhang et al., 2016) *WHY1* genomic sequence in Geneious Prime using Minimap2 (version 2.17, Li, 2018) with a K-Mer length set to 15.

FIGURE 1

Overview of *Corallorhiza* species included in this study, showing plastid and nuclear phylogenetic relationships, inflorescence, trophic status (fully vs. partially mycoheterotrophic), plastome size (bp), number of putatively functional plastid genes, and chlorophyll content (mean and standard deviation in nanograms of total chlorophylls per milligram of plant material). Phylogenetic, plastome, and chlorophyll content data are from Barrett et al. (2014).

2.6 Alignment

We aligned all *Corallorhiza WHY1* isoforms using MAFFT (version 7.3.10; Katoh and Standley, 2013), and the E-INS-i algorithm (Katoh et al., 2002) and the 1PAM scoring matrix, as a Geneious Prime plugin. Visualization and structural annotation against the canonical *WHY1* sequence of *Arabidopsis thaliana* (NCBI Q9M9S3) was also conducted using Geneious Prime. Consensus was determined as majority consensus with a 0% threshold, meaning no minimum frequency was required for a consensus character if the character was shared by most sequences. All *Corallorhiza WHY1* isoforms were translated in Geneious Prime to amino acid sequence and manually trimmed to the correct ORF. ORF-trimmed *WHY1* translations were aligned with the ORF-trimmed *WHY1* sequence of *Arabidopsis thaliana* (NCBI NM101308) to verify the presence of the expected canonical reading frame.

A translation-aware alignment of the canonical form of *WHY1* representing lineages across the angiosperms was generated using a two-step process. Nucleotides were first aligned and translated using the frameshift-aware aligner MASCE2 (version 2.0.6; Ranwez et al., 2011) with default parameters, which inserts gap characters necessary to maintain codon-based statements of homology across the alignment. This approach was necessary due to the presence of frameshift mutations in sequences from *Gastrodia elata*, *Epipogium aphyllum*, and *C. striata*. The MACSE2-processed nucleotide and amino acid alignments were then refined using MAFFT and the E-INS-i algorithm with a BLOSUM 80 substitution matrix.

An alignment including the complete genomic sequences of *WHY1* from *Phalaenopsis equestris* (ASM126359v1) and *Dendrobium catenatum* (ASM160598v2) was also generated. *Phalaenopsis equestris* (Cai et al., 2015) and *D. catenatum* (Zhang et al., 2016) are the closest relatives of *Corallorhiza* with sequenced genomes (Chen et al., 2022). This DNA alignment was generated to identify the introns of *WHY1* and to evaluate the exonic content of assembled transcripts. All *Corallorhiza* isoforms and *Corallorhiza* Nanopore consensus sequences were aligned with the sequences of *P. equestris* and *D. catenatum* using MAFFT (version 7.3.10; Katoh and Standley, 2013), as a Geneious Prime plugin, and the E-INS-i algorithm (Katoh et al., 2002).

2.7 Visual screening for amino acid substitutions

Nonsynonymous substitutions within the angiosperm *WHY1* alignment were surveyed visually in our amino acid alignments via Geneious Prime. Substitutions of interest included those present exclusively in *Corallorhiza* species, mycoheterotrophs, and the Orchidaceae. The codons of *A. thaliana* (Q9M9S3) and *P. equestris* that corresponded to the sites of nonsynonymous substitutions in *WHY1* of interest were cross-referenced with the annotated *A. thaliana WHY1* sequence for structure and the *P.*

equestris WHY1 genomic sequence as included in the DNA alignment for exon location.

2.8 Phylogenetic inference

IQ-TREE (version 1.6.12; Nguyen et al., 2015) was used to infer phylogenetic relationships among the recovered *WHY1* sequences using automated model choice (Kalyaanamoorthy et al., 2017), optimal partitioning assessment (Chernomor et al., 2016), and nearest neighbor interchange search enabled. Node support was estimated using 1,000 ultrafast bootstrap approximation replicates (Hoang et al., 2018). Two partitions were defined, which comprise the signal peptide and the highly variable 5' portion of the chain (positions 1–516) and the highly conserved chain region (517–1,122), identified using functional annotations on *WHY1* sequence per *A. thaliana* (Q9M9S3). The *Amborella trichopoda WHY1* sequence was used for phylogram rooting.

2.9 Selection analyses

The *WHY1* nucleotide alignment was tested for statistically significant changes in selection regime using four methods implemented in the command-line, multithreaded version of the Hypothesis Testing using Phylogenies suite (HyPhy; version 2.5.39; Pond and Muse, 2005). We used the Genetic Algorithm for Recombination Detection (GARD; Pond et al., 2006), with default parameters, to test for signal of recombination breakpoints within *WHY1*. We tested for significant change of selective regime using five test branch sets against null reference branch sets comprising all other species in the phylogram: (1) *Corallorhiza* species; (2) *C. maculata + C. striata*; (3) *Corallorhiza + Epipogium aphyllum + Gastrodia elata*; (4) *C. maculata + C. striata + E. aphyllum + G. elata*; (5) *E. aphyllum + G. elata*. The same *Amborella trichopoda*-rooted maximum likelihood *WHY1* topology inferred with IQ-tree was used for all analyses.

RELAX (Wertheim et al., 2015) was used to test for evidence of relaxed selection. RELAX breaks each codon into its three component sites, each with an assigned omega class. Values for omega are calculated as Dn/Ds ratios, using the calculation for the reference branches as the null hypothesis. The value k is the selection intensity parameter and is an exponent value on omega. The alternative model fits a value for k that changes the rate to fit with the test branches. Evidence for intensified selection strength along test branches is indicated by a significant result where the value of k is greater than 1 ($k > 1$, $P < 0.05$). Evidence for relaxed selection along test branches is indicated by a significant value of k less than 1 ($k < 1$, $P < 0.05$). Strength of selection was assessed simultaneously for all species using Fast Unconstrained Bayesian Approximation (FUBAR, Murrell et al., 2013). FUBAR can detect weak, yet pervasive, purifying or diversifying selection at the codon level (posterior probability >0.90) without the use of test and reference branch sets.

The Branch-Site Unrestricted Statistical Test for Episodic Diversification (BUSTED) was used to test for evidence of gene-wide positive selection (Murrell et al., 2015). BUSTED uses three omega classes defined as ω1 ≤ ω 2 ≤ 1 ≤ ω3. The ω1 class is the proportion of sites with a very low Dn/Ds ratio. The ω2 class is the proportion of sites just below 1, and ω3 are sites above 1. A value of 1 suggests selective neutrality, and therefore defines the null, or constrained, model. BUSTED then calculates the log-likelihood of the data for each of the null and alternative models. These ratios are calculated for each site and are called evidence ratios (ERs). They are used as a threshold (χ^2 distribution, $P < 0.01$) but are not a valid test for site-specific likelihood. The null model is rejected if at least one site on a test branch experienced positive selection. Evidence for positive, or diversifying, selection in a gene of a test branch is indicated by a rejection of the null model.

The adaptive branch-site random effects likelihood (aBSREL) test was used to test for signal of episodic positive selection. aBSREL infers ω values at both the level of sites and branches and can account for rate heterogeneity inherent to complex evolutionary scenarios by partitioning these values into multiple rate classes per branch. aBSREL was conducted in exploratory mode, where all branches were tested and *p*-values were Holm–Bonferroni corrected, and in the more sensitive *a priori* mode to test for episodic positive selection in each test branch set.

3 Results

3.1 *De-novo* assembly and identification of *WHY1*

The hmmer suite revealed a single, Trinity-identified gene model and its isoforms as representing *WHY1* from *de-novo* assembled transcripts for each *Corallorhiza* species. Trinity assembled a single isoform representing the expected canonical CDS (coding DNA sequence) of *WHY1* for all but *C. striata*, the latest stage fully mycoheterotrophic species of *Corallorhiza* sampled. However, mapping reads to each isoform with BBMAP revealed that a five nucleotide indel, the absence of which results in a premature stop codon, was differentially present or absent in the reads of each *Corallorhiza* species (NCBI BioProject PRJNA984634). Trinity differentially incorporated that indel, hereafter referred to as the GTGAA indel, into the isoform pool of each *Corallorhiza* species. The absence of the GTGAA indel in Trinity-assembled isoforms of *C. striata* precluded the recovery of the canonical ORF, but read mapping supports the presence of the five nucleotides necessary to recover the expected ORF in *C. striata*, at a rate of 67.2% of reads in isoform 2 and 76.1% of reads in isoform 4. Those data support that the canonical variant of *WHY1* is also expressed. We analyzed the *C. striata* isoforms as assembled, rather than manually modifying the *C. striata* transcripts to conform to a hypothesized canonical sequence. The inclusion of those five nucleotides would not alter any results presented here, aside from whether a canonical *WHY1* isoform is transcribed in *C. striata*.
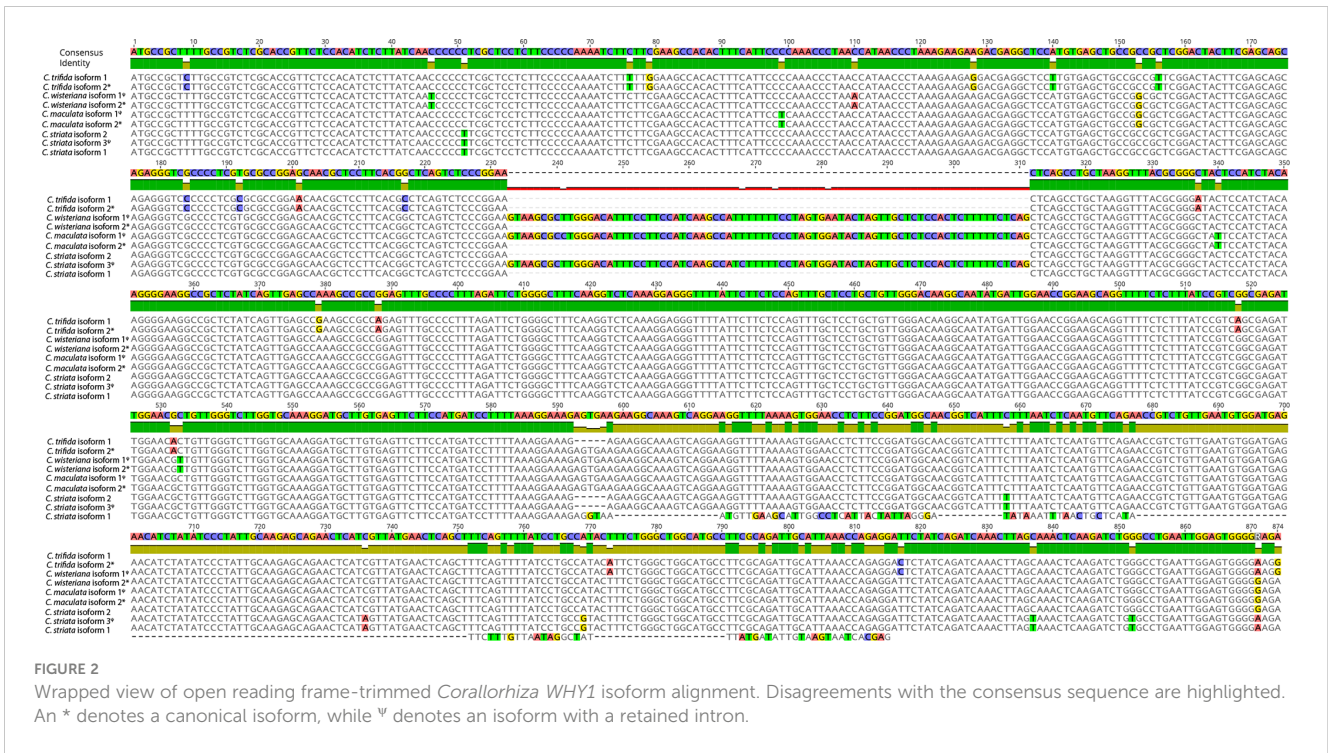
The canonical *WHY1* ORF as assembled in *C. trifida*, *C. wisteriana*, and *C. maculata* is 795 nucleotides in length and comprises 265 amino acids, two fewer amino acids than that of *A. thaliana*. Non-canonical splicing variants were found in the isoform pools of each *Corallorhiza* species. A splicing variant containing a 79-nucleotide long sequence of 96.6% mean pairwise identity was recovered from *C. wisteriana*, *C. maculata*, and *C. striata*, at nucleotide position 232. The second major variant is the GTGAA indel discussed earlier, which is variously present at nucleotide position 514 in all four species. A third variant identified from the isoform pool of *C. striata* represents a modification of the 3' end of the ORF, immediately downstream of the previously discussed five-nucleotide indel that was variously present in our read pools throughout *Corallorhiza*.

3.2 Alignment

MAFFT alignment of all raw Trinity-assembled *Corallorhiza WHY1* isoforms resulted in a matrix of 1,302 positions. Pairwise percent identity across isoforms was 81.4% and 88.2% and gaps comprised 11.7% and 8.1% of character states for all isoforms and with the exclusion of the early terminating isoform 1 of *C. striata*, respectively. Alignment of ORF-trimmed transcripts resulted in a matrix of 874 positions (Figure 2). Percent pairwise identity among isoforms within a species was highest for *C. trifida* (99.5%) and lowest for *C. striata* (70.6%). A 79-nucleotide-long indel of 96.6% pairwise identity was identified in at least one isoform assembled from all *Corallorhiza* species except *C. trifida*. Translation-aware alignment of ORF-trimmed canonical *Corallorhiza WHY1* sequences, with the differentially present GTGAA indel manually inserted into the otherwise canonical sequence of *C. striata*, resulted in an alignment of 795 characters of 98.0% pairwise identity and no gaps. The highest pairwise percent identity was 99.37% between *C. wisteriana* and *C. maculata* and the lowest was 96.98% between *C. trifida* and *C. striata*.

The *WHY1* genomic DNA alignment of *Corallorhiza* isoforms, *Corallorhiza* Nanopore sequences, and *P. equestris* and *D. catenatum* genomic sequences had a total length of 12,000 nucleotides (Figure 3), in which the assembled canonical isoforms from each *Corallorhiza* species contained the expected exons of *WHY1*. One non-canonical isoform of *C. wisteriana*, *C. maculata*, and *C. striata* each contained intron 1, for which pairwise percent identity was 96.6% across those species. Percent pairwise identity of intron 1 between that of *D. catenatum* and *P. equestris* was 82.3%, and similarity between retained introns and that of *P. equestris* ranged from 78.5% to 82.3% for *C. maculata* and *C. striata*, respectively. The Nanopore-sequenced and Trinity-assembled *WHY1* intronic sequences of *C. striata* were identical, while those of *C. maculata* were 94.9% similar, due to the relative lack of two thiamine nucleotides in the Nanopore sequence.

The angiosperm-scale *WHY1* nucleotide alignment contained *WHY1* sequences from 110 species, including 22 orchid species. The total length of the alignment was 1,122 positions, of which 150 were of identical states across all species. Two partitions roughly

FIGURE 2
Wrapped view of open reading frame-trimmed *Corallorhiza WHY1* isoform alignment. Disagreements with the consensus sequence are highlighted. An * denotes a canonical isoform, while Ψ denotes an isoform with a retained intron.
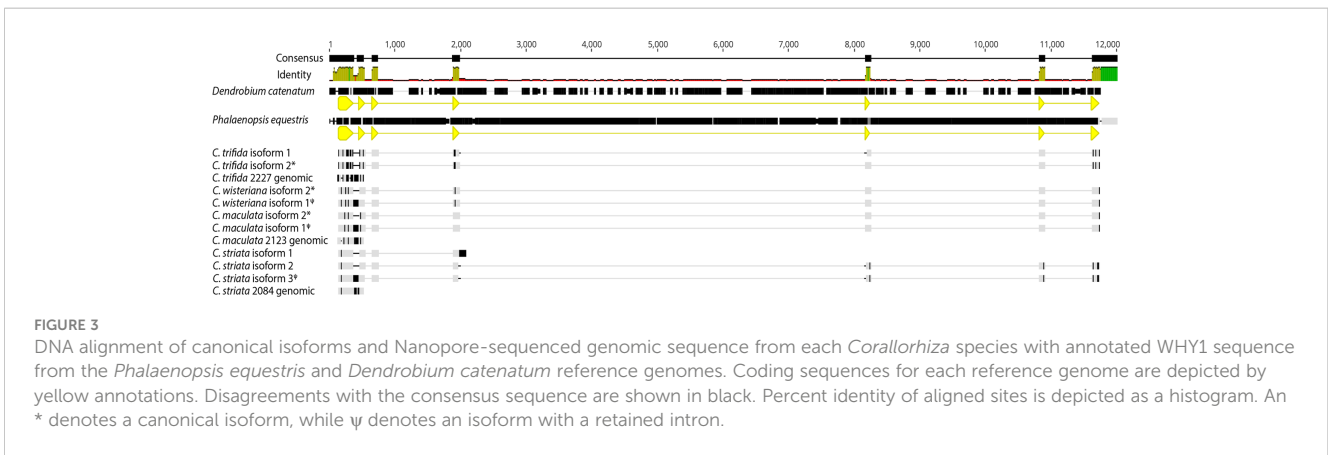
corresponding to the transit peptide and chain regions as annotated in *A. thaliana* (Q9M9S3) were conspicuously visible in the consensus sequence of the alignment. The first was a highly variable, lineage-specific portion of sequence ranging from positions 1–516 in the alignment. The second was a highly conserved portion spanning positions 517–1,122. The mean pairwise percent identity of the transit region of Orchidaceae was 51.3%, while that of *Apostasia shenzhenica* compared to either *G. elata* or *E. aphyllum* was 21.5% and 31.1%, respectively. The mean pairwise percent identity of the transit region of *Corallorhiza* was 94.4%. The mean pairwise percent identity of the four *Corallorhiza* species in the alignment was 97.7% and 81.0% across the Orchidaceae. The grasses had the lowest mean percent pairwise similarity of any clade, which was 49.36% when each sequence was compared to each non-grass species in the alignment.

The angiosperm-wide *WHY1* amino acid alignment comprised 376 positions, of which 48 were of identical states across all species.

The two partitions in the nucleotide alignment corresponding to functional annotation in *A. thaliana* (Q9M9S3) were more conspicuous in the amino acid alignment. Positions 1–115 and 116–376 corresponded to the transit and chain regions of *A. thaliana* (Q9M9S3), respectively. The pairwise percent identity of the four *Corallorhiza* species in the alignment was 97.4% for *WHY1*, and across the Orchidaceae it was 77.8%.

3.3 Nanopore sequencing

Nanopore sequencing of genomic *WHY1* sequence from three of the four *Corallorhiza* species confirmed that the unique sequence in the non-canonical transcripts of *C. wisteriana*, *C. striata*, and *C. maculata* represented retention of *WHY1* intron 1. Sequencing of *WHY1* amplicons generated read pools ranging from 25,546 to 74,261 reads in *C. trifida* and *C. maculata*, respectively. Mapping of

FIGURE 3
DNA alignment of canonical isoforms and Nanopore-sequenced genomic sequence from each *Corallorhiza* species with annotated WHY1 sequence from the *Phalaenopsis equestris* and *Dendrobium catenatum* reference genomes. Coding sequences for each reference genome are depicted by yellow annotations. Disagreements with the consensus sequence are shown in black. Percent identity of aligned sites is depicted as a histogram. An * denotes a canonical isoform, while ψ denotes an isoform with a retained intron.

Nanopore reads against the *D. catenatum* genomic *WHY1* sequence resulted in a mean coverage depth for the exon 1–2 region ranging from 4,034.9 to 10,617.6 in *C. trifida* and *C. striata*, respectively (Supplementary Table S2). Library preparation for Nanopore sequencing of *C. wisteriana WHY1* amplicons was deemed unsuccessful since the resulting sequence pool contained presumably off target reads that precluded confident assembly of a *WHY1* consensus sequence from that sample. Alignment of the Nanopore-sequenced *WHY1* amplicon consensus reads with the *Corallorhiza* transcript isoforms and the full *WHY1* genomic sequences of *P. equestris* and *D. catenatum* provided evidence that the non-canonical isoforms of *WHY1* in *Corallorhiza* were a result of alternative splicing (Figure 4). At least one non-canonical isoform from all but *C. trifida* contains intron 1 of *WHY1*.

The sequences obtained from *Corallorhiza* species via Nanopore and RNA-seq shared a high degree of similarity with each other and the *WHY1* sequence in the previously published *P. equestris* and *D. catenatum* genomes. Intron 1 of *WHY1* was found to have a pairwise percent similarity of 82.3% between *P. equestris* and *D. catenatum*. *Corallorhiza WHY1* intron 1 sequences obtained via Nanopore sequencing and RNA-seq had a mean pairwise percent similarity of 96.9%, while that of *C. striata* obtained via both RNA-seq and Nanopore sequencing had a pairwise percent similarity of 82.3% with *P. equestris*.

3.4 Select amino acid substitutions of interest

Substitutions exclusive to mycoheterotrophic species were evident and, in some cases, were exclusive to fully mycoheterotrophic species. The transit regions of both *E. aphyllum* and *G. elata* contained some substitutions that were unique within the Orchidaceae. A phenylalanine-glycine residue at positions 76–77 was exclusive to *C. trifida*, while a leucine-arginine residue was present for the remainder of Orchidaceae at those positions. While pairwise percent identity of positions 76–77 was only 13.3% throughout angiosperms, the leucine-arginine residue in the Orchidaceae had a pairwise percent identity of 90.9% when including the residue from *C. trifida* and was identical when that taxon was excluded. Amino acid substitutions found in the transit regions of both *C. wisteriana* (positions 46 and 95) and *C. trifida* (position 113) were not identified in other orchids but were found in some non-orchid autotrophs.

At least one substitution that could impact *WHY1* conformation was identified in *Corallorhiza*. The terminal codon of an alpha helix annotated in the structure of *A. thaliana* (9M9S3) *WHY1* (position 336) has been substituted to an isoleucine in *C. trifida* and to a phenylalanine in *C. wisteriana*, *C. maculata*, and *C. striata* (Figure 5). We infer that the ancestral state of position 336 is leucine, on the basis of that codon state for 89.1% of sampled taxa, including *Amborella*

FIGURE 4

DNA alignment of *Corallorhiza* isoforms assembled from each *Corallorhiza species* and Nanopore sequences for *C. trifida*, *C. maculata*, and *C. striata* with annotated *WHY1* sequence from the *Phalaenopsis equestris* and *Dendrobium catenatum* reference genomes. *WHY1* exons 1 and 2 are annotated in yellow and the locus ID tags for each reference genome are provided in the coding sequence (yellow) annotations. Disagreements with the consensus sequence are highlighted. Percent identity of aligned sites is depicted as a histogram. An * denotes a canonical isoform, while Ψ denotes an isoform with a retained intron.
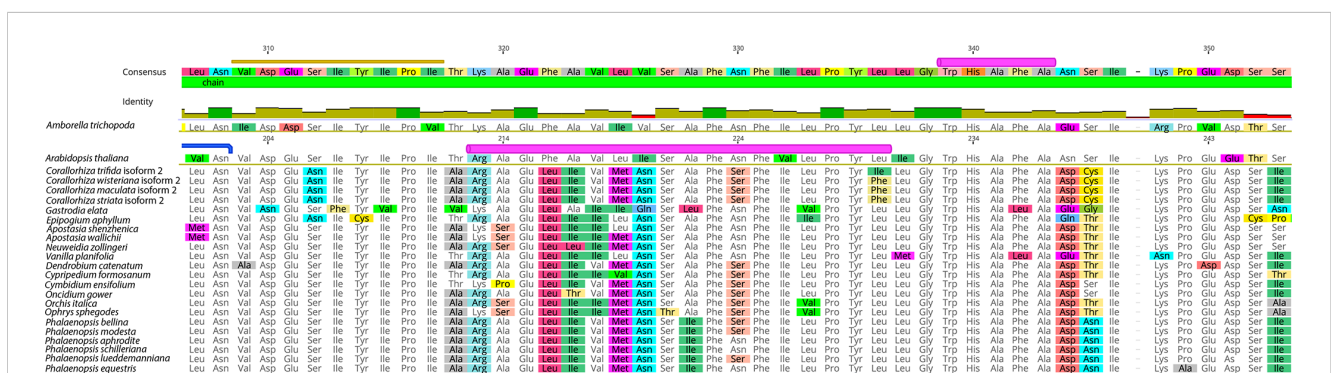

FIGURE 5

Detailed view of amino acid alignment of *WHY1* sequences of orchid species. Note the phenylalanine substitutions unique to *Corallorhiza wisteriana*, *C. maculata*, and *C. striata*, relative to the other species sampled. The amino acid substitutions of interest are located at the 3′ portion of a region inferred to conform into an alpha helix structure (pink annotation) in *Arabidopsis thaliana WHY1* (alignment row two).

trichopoda. The only other substitutions at that position were to isoleucine, which was identified in eight autotrophic angiosperms outside the Orchidaceae, and in *C. trifida*. Additionally, a substitution from alanine to valine at position 359 was exclusive to *C. striata*, which represents the only occurrence of that state for this position for 109 other angiosperm species, and the only subgeneric polymorphism observed in that position.

A five-nucleotide indel resulting in a frameshift (amino acid alignment positions 269 and 270) was found in *C. striata*, but the pairwise percent identity of downstream sequence with that of *C. maculata* was high (97.8%) and reads containing the corresponding five nucleotides were identified in the RNA-seq read pool. In fact, RNA-seq reads containing the indel were found in the read pools of all *Corallorhiza* species, suggesting that isoform diversity was conservatively interpreted by our methods.

We found that the chain region of *E. aphyllum* contained a glycine to arginine substitution in the characteristic *WHY1* ssDNA-binding motif (positions 188–193), a site that was otherwise conserved throughout the remainder of samples. Additionally, we found that the *E. aphyllum* sequence contained a residue comprising seven amino acids (positions 294–300), the last of which was a premature stop codon. MAFFT resolved those seven amino acids as an insertion with no homology to other angiosperm sequences. Six substitutions downstream of that premature stop codon are exclusive to *E. aphyllum*.

3.5 Phylogenetic inference

Both the Eudicots and Monocots were recovered as monophyletic (Figure 6; BS = 100%). Orchidaceae was recovered as a monophyletic group (BS = 94%), with *D. catenatum*, *G. elata* and *E. aphyllum* as an early diverging paraphyletic grade within the Epidendroids (BS = 98%). However, the positions of *D. catenatum* (BS = 79%) and *G. elata* (BS = 76%) were not robustly supported. *Corallorhiza* species were recovered as a monophyletic group (BS = 100%) with *C. trifida* sister to *C. striata* (BS = 100%) + (*C. wisteriana*, *C. maculata*; BS = 100%), rather than those inferred in previous, genomic-scale work depicted in Figure 1.

3.6 Differential expression

Canonical isoforms of *WHY1* were most highly expressed in all four species (see Table 1), but statistically significant elevated expression in aboveground tissues relative to those belowground was only detected in *C. trifida*. Gene-level expression of *WHY1* across both tissues was highest for *C. wisteriana* (244.5) and *C. trifida* (175.4) and lowest for *C. maculata* (131.9) and *C. striata* (95.3). Expression of the canonical isoform of *WHY1* in *C. trifida* ranged from 4.15 to 9.64 TMM in belowground tissues (median = 7.17 TMM) and from 31.353 to 56.389 TMM in the aboveground tissues (median = 43.273 TMM). The log fold-change value was 2.56 between belowground and aboveground tissues for the canonical isoform of *C. trifida*, with a *P*-value of 0.00018 and a false discovery rate (FDR) of 0.00374. Expression of the *WHY1* nearly canonical isoform in *C.*
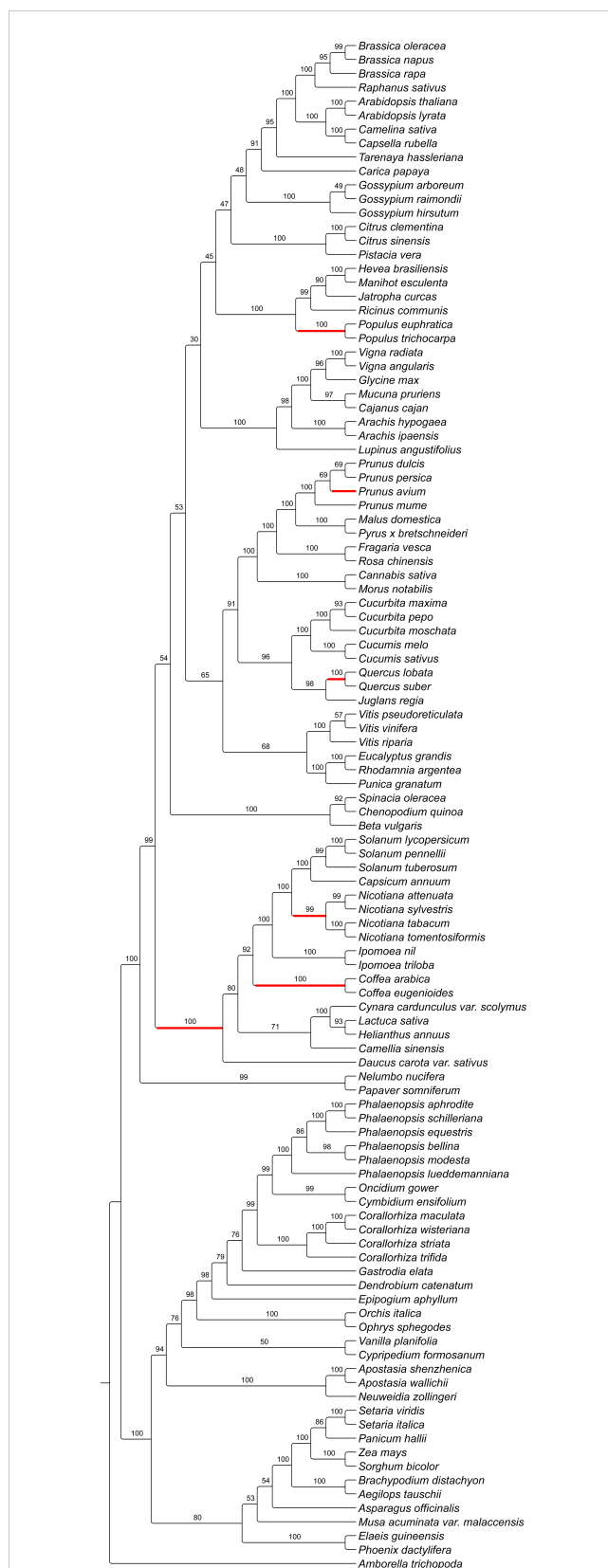

FIGURE 6
Maximum likelihood inferred topology of *WHY1* evolution with support values derived from 1,000 non-parametric bootstrap replicates. Lineages highlighted in red represent those for which statistically significant signal of episodic diversifying selection of *WHY1* was detected by the adaptive branch-site random effects likelihood test.

TABLE 1 *In silico* expression of *WHY1* across species, tissues, and biological replicates.

Species gene or isoform	Belowground tissue (biological replicate #)			Aboveground tissue (biological replicate #)			Log_FC	P-value (Q-value)
C. trifida	1	2	3	1	2	3		
Gene	12.7	11.6	4.7	31.4	71.0	43.7	2.12	0.004 (0.057)
Isoform 1	5.0	1.8	1.0	1.4	2.9	4.3	0.12	0.915 (0.998)
Isoform 2*	7.7	9.6	4.1	31.3	56.3	42.0	2.56	0.0001 (0.003)
C. wisteriana	1	2	3	1	2	3		
Gene	14.2	23.0	8.3	84.3	76.7	37.8	1.91	0.019 (0.176)
Isoform 1$^\Psi$	0	0.8	0	1.0	1	2.0	2.36	0.313 (1)
Isoform 2*	14.7	23.0	9.2	74.9	72.6	34.7	1.96	0.021 (0.283)
C. maculata	1	2	NA	1	2	3		
Gene	16.6	12.7		47.0	25.3	30.0	1.17	0.162 (0.624)
Isoform 1$^\Psi$	2.0	1.8		0.5	0	3.5	−0.51	0.746 (0.970)
Isoform 2*	13.9	11.0		45.9	26.1	26.8	1.33	0.119 (0.387)
C. striata	1	2	3	1	2	NA		
Gene	21.3	16.4	7.8	32.1	17.3		0.62	0.525 (0.804)
Isoform 1	0.9	0	2.3	0	0		NA	NA
Isoform 2	16.8	14.5	5.5	30.5	17.2		0.39	0.695 (0.918)
Isoform 3$^\Psi$	4.4	0.7	0.5	0.8	0		−2.88	0.254 (0.536)

The first row for a species contains values for gene-level expression, while subsequent rows contain values for a specific isoform. Trinity isoform and biological replicate identifiers are provided in Supplementary Table S3. Expression values are trimmed-mean-of-means-transformed (TMM) transcripts per million (TPM) in order to maintain comparability among biological replicates. An * denotes a canonical isoform, while $^\Psi$ denotes an isoform with a retained intron. Values shown have been truncated, TMM to the tenth, LogFC to the hundredth, and P- and Q-values to the thousandth.

striata ranged from 5.547 to 16.859 TMM in belowground tissues (median = 12.31 TMM) and 17.28 and 30.538 TMM in aboveground tissues (median = 23.909 TMM). The *C. striata* canonical *WHY1* isoform had a log fold-change value of 0.396 between belowground and aboveground tissues, with a *P*-value of 0.69 and FDR of 0.91. Expression of the canonical isoform of *WHY1* in *C. wisteriana* ranged from 9.256 to 23.023 TMM in belowground tissues (median = 15.663 TMM) and 34.792 to 74.955 TMM in aboveground tissues (median = 60.80 TMM). The *C. wisteriana* canonical isoform had a log fold-change value of 1.96 between belowground and aboveground tissues, with *P*-value of 0.02 and FDR of 0.28. The expression of the canonical isoform in *C. maculata* had values of 11.064 and 13.947 TMM in belowground tissues (median = 12.51 TMM) and ranged from 26.179 to 45.999 TMM in aboveground tissues (median = 33.01 TMM). The *C. maculata* canonical isoform had a log fold-change value of 1.17 between belowground and aboveground tissues, with *P*-value of 0.16 and FDR of 0.62.

The expression of non-canonical isoforms assembled from the read pools of all four species varied across tissues and samples, with some tissues or individuals not expressing splicing variants, and expression was not statistically different between the two tissue types in any of the four species. The *C. trifida* non-canonical isoform was expressed at relatively low levels across all aboveground and belowground tissues, the TMM of which ranged from 1.02 belowground to 4.374 aboveground. Contrastingly, the TMM of the *C. wisteriana* non-canonical isoform ranged from 0 to 2.017 and was not detected in two of the belowground replicates for this species. The noncanonical *C. maculata* and *C. striata* isoforms were sporadically expressed across tissue types, with the TMM values of one isoform of *C. maculata* ranging from 0 to 3.564 and those of *C. striata* ranging from 0 to 4.471. Even in the case of the *C. striata* isoform for which the TMM value was 4.471 in one belowground sample, the value was either 0 or less than 1 in the remainder of samples.

3.7 Selection analyses

GARD evaluated 2,393 models and inferred a single potential recombination breakpoint, separating the signal peptide and chain portions of *WHY1*, but AIC$_c$ was not significantly improved for the partitioned analysis (75,130.4) versus unpartitioned (75,111.5). The RELAX test inferred statistically significant signal for relaxation of selection pressure for the following test branch sets: *Corallorhiza* + *E. aphyllum* + *G. elata* ($p = 0.001$); *C. maculata* + *C. striata* + *E. aphyllum* + *G. elata* ($p = 0.002$); and *E. aphyllum* + *G. elata* ($p = 0.001$). However, runs of RELAX analyzing test branch sets comprising only *Corallorhiza* ($p = 0.30$) or *C. maculata* + *C. striata* ($p = 0.62$) did not infer significant signal for selection relaxation.

The FUBAR analysis inferred that 254 of 373 codons were under pervasive purifying selection (posterior probability threshold ≥0.9) and that no codons were under pervasive diversifying selection. Likewise, the BUSTED analyses did not infer statistically significant signal of gene-wide episodic diversifying selection for any test branch set, where *p*-values ranged from $p = 0.15$ for *E. aphyllum* + *G. elata* to $p = 0.50$ for *Corallorhiza*.

The aBSREL analysis recovered signal of episodic diversifying selection in seven of 217 branches in the *WHY1* tree (Figure 6) but did not infer statistically significant signal in any test branch set during analyses conducted in *a priori* mode. The terminal node leading to *Sorghum bicolor* ($p = 2.76 \times 10^{-6}$) was the only branch in the monocots that showed significant signal of episodic diversifying selection. Within the eudicots, the branches leading to *Prunus avium* ($p = 2.5 \times 10^{-5}$), the *Populus* clade ($p = 1.17 \times 10^{-7}$), the *Quercus* clade (2.35×10^{-3}), the *Nicotiana* clade ($p = 5.42 \times 10^{-3}$), the *Coffea* clade (6.96×10^{-5}), and the asterid clade ($p = 3.7 \times 10^{-4}$) were inferred to contain signal of episodic diversifying selection.

4 Discussion

Our work represents the largest scale investigation of *WHY1* evolution to date and reveals strong phylogenetic signal for this gene across multiple taxonomic levels in the angiosperms. Phylogenetic methods have emerged as the gold-standard for the inference of gene orthology (Münster et al., 1997; Emms and Kelly, 2015, Emms and Kelly, 2019) by which hundreds of genes have been determined to not only be highly conserved across plant lineages but to exist as low- or single-copy (Wu et al., 2006; Duarte et al., 2010; De Smet et al., 2013). The inferred evolutionary relationships of *WHY1* (Figure 6) were largely congruent with our contemporary understanding of angiosperm phylogenetic relationships and recent inferences based on genomic-scale datasets (The Angiosperm Phylogeny Group, 2016; Guo et al., 2021; Zhao et al., 2021). Likewise, the inferred relationships within the Orchidaceae were largely consistent with those inferred in other studies (e.g., Givnish et al., 2016; Li et al. 2019; Pérez-Escobar et al., 2021; Serna-Sánchez et al., 2021; Zhang et al., 2023; Barrett et al., 2024; Pérez-Escobar et al., 2024), apart from *D. catenatum*, *G. elata*, and *E. aphyllum* forming an early diverging, paraphyletic grade within the

Epidendroids. However, our recovery of *C. trifida* as sister to the remainder of the species sampled from *Corallorhiza*, rather than *C. striata*, was not congruent with relationships inferred previously on the basis of other loci and even genomic-scale datasets (Barrett and Freudenstein, 2008; Barrett et al., 2014, Barrett et al, 2018). We are not surprised to infer discordance between the evolutionary history of *WHY1* and that of the phylogenetic history of *Corallorhiza*, since it is accepted that the evolutionary history of any gene can differ from that of the genome within which it is found (Pamilo and Nei, 1988; Maddison, 1997). That said, the recovery of the *Corallorhiza* species with the most intact plastome as sister to those with more degraded plastomes may indicate that the gene-species tree discordance we infer is due to functional convergence in *WHY1* sequence. For example, the phenylalanine substitution at position 336 shared by all *Corallorhiza* species aside from *C. trifida* may affect protein conformation and therefore *WHY1* function. Our findings of general congruence between the evolutionary history of *WHY1* across angiosperms supports the gene as single- or low-copy across the 110 angiosperm taxa sampled.

Differences in the degree of nucleotide conservation were evident among *WHY1* exons, with the transit peptide region consistently the most divergent throughout the lineages sampled. The diversity and evolution of transit peptides, and the apparent discrepancy between our perception of their functional importance and high-sequence divergence, have long been of interest (Bruce, 2001; Patron and Waller, 2007; Christian et al., 2020). While the functional nature of a transit peptide might lead to an expectation of conservatism, low-sequence similarity and patterns of mutation that we describe in *WHY1* are emerging as generalizable properties of plant transit peptides. For example, Christian et al. (2020) found that the transit peptides in the genomes of 15 genera sampled throughout the angiosperms had a mean pairwise percent identity of just 37.9% and that random indels drive transit peptide evolution. Our results provide evidence that the transit peptide of *WHY1* evolves similarly, with a pairwise percent identity of 32.5% across the angiosperms, and with evident substitutions and indels downstream of a homologous start codon being the most likely drivers of divergence in the gene region. In contrast, the portion of the chain encoding the ssDNA binding motif was the most conserved with a mean percent pairwise similarity of 72.1%. The only sizable indel observed in the gene region was a seven-codon insertion in *E. aphyllum*, a late-stage mycoheterotrophic orchid. It is likely that *E. aphyllum WHY1* results in a non-functional product, given that it encodes a premature stop codon that would result in a protein 70 amino acids shorter than that of any other sampled species. Interestingly, *WHY1* was more conserved overall at the nucleotide level among *Corallorhiza* species than were either expression patterns across tissues or exon inclusion in sequenced mRNAs across the trophic gradient. Among autotrophic species, nucleotide divergence of *WHY1* is particularly pronounced in the grasses, with the mean pairwise percent identity among all members of that clade versus the remainder of samples being more than 5% lower than that of the same comparison made for either of the late-stage mycoheterotrophic species sampled. The high substitution rate we inferred for *WHY1* in the grasses is interesting because the

plastomes of many species in the clade are known to contain inversions and structural heteroplasmy within individual plants, of which the latter has only recently been described from their relatives the Cyperaceae (Doyle et al., 1992; Lee et al., 2020). The contrasting levels of nucleotide conservation in the transit and chain portions of *WHY1* across lineages suggest that lineage-specific functions of the transit peptide sequence could be a fruitful line of investigation, especially given that Christian et al. (2020) identified bias in amino acid usage between the plastid transit peptide sequences of monocot and eudicot lineages.

Alignment of *WHY1* revealed lineage-specific substitutions at sites inferred to be involved in structural conformation in both poorly and highly conserved gene regions. For example, the transit regions of both late-stage mycoheterotrophic species contained indels not found in other samples, and the sequence of *E. aphyllum* contained a premature stop codon in the typically highly conserved chain region followed downstream by four autapomorphic amino substitutions in an eight amino acid span. We identified substitutions that could underlie functional change in each *Corallorhiza* species, the most interesting of which was a substitution involving an alpha helix (position 336) inferred in previous work conducted in *A. thaliana* (Cappadocia et al., 2013). Our phylogenetic framework supports the plesiomorphic codon state of position 336 as a leucine, which we infer was substituted to a phenylalanine in *Corallorhiza* and then to an isoleucine in *C. trifida*, on the basis of the relationships depicted in Figure 1. We additionally infer that the phenylalanine substitution present in *Corallorhiza* species aside from *C. trifida* would result in the introduction of a benzene ring in which there were previously only aliphatic hydrocarbons. However, comprehensive taxonomic sampling of *WHY1* across *Corallorhiza* is needed to determine sequence diversity and substitution patterns. While our work revealed many nonsynonymous substitutions throughout *Corallorhiza* sequences, we did not identify nucleotide substitutions that obviously result in loss of function in these transitional mycoheterotrophic species.

Statistically significant shifts of selective regime were detected for late-stage mycoheterotrophic and some non-orchid autotrophic lineages. Our inference that 68.1% of *WHY1* codons are under pervasive purifying selection and none are under pervasive positive selection, despite the relatively low levels of nucleotide conservatism we documented, are congruent with the critical function of the gene across the angiosperms as has been documented in model and agricultural species in previous work (Cappadocia et al., 2013; Lepage et al., 2013; Zampini et al., 2015; Ren et al., 2017; Qiu et al., 2022; Ruan et al., 2022; Taylor et al., 2022; Sun et al., 2023). While we inferred disproportionately high substitution rates for *WHY1* in the grasses, we did not find evidence that divergence of those sequences was associated with diversifying selection. Despite the lack of pervasive positive selection in *WHY1* across the angiosperms, our identification of significant episodic diversifying selection in seven of 100 autotrophic lineages sampled suggests that a lineage-specific adaptive role of *WHY1* may be relatively common, though similar signal was not identified in sampled mycoheterotrophs. The lack of diversifying signal in any of our mycoheterotrophic species does not support neofunctionalization

of the gene, which we find interesting given the multiple functions of *WHY1* and the diversifying signal identified in lineages across the angiosperms. Our findings together suggest that relaxation of *WHY1* selective constraint occurs after the transition to full mycoheterotrophy, as significant signal of relaxed selection was only detected in branch sets containing *E. aphyllum* and *G. elata*, two late-stage fully mycoheterotrophic orchids.

Our analyses suggest that the expression of *WHY1* in *Corallorhiza* may differ by both tissue type and across the mycoheterotrophic gradient. Multiple studies have induced and characterized the effects of differential expression of *WHY1* by exposure to biotic and abiotic stimuli, implicating roles for the gene ranging from mediating drought stress (Zhao et al., 2018; Ruan et al., 2022) to pathogen response (Desveaux et al., 2000; Sun et al., 2023). A minimum level of *WHY1* expression could be expected due to roles of *WHY1* that are not involved in photosynthesis, such as the maintenance of telomere length of nuclear chromosomes (Yoo et al., 2007). Our analyses are the first to characterize *WHY1* expression in non-model or non-cultivated plant species, and therefore baseline expectations for tissue-specific expression levels for wild species have not yet been established. However, the estimations of gene expression we inferred for *Corallorhiza* species are within the expression ranges reported in studies of *A. thaliana* (4–76 TPM; Liu et al., 2012; Mergner et al., 2020) and *Solanum tuberosum* (7–50 TPM; The Potato Genome Sequencing Consortium, 2011). Additionally, the Klepikova *Arabidopsis* Atlas (Klepikova et al., 2016) and 1,122 tissue-specific samples available via the *Arabidopsis* RNA-seq Database (http://ipf.sustech.edu.cn/pub/athrdb/ accessed 8 March 2023) evidence that *WHY1* expression should be expected to be lower in roots or rhizomes than in leaves, which is congruent with expression patterns in *C. trifida*. Previous studies reporting *WHY1* expression have been conducted in species with larger individuals with typical, non-reduced morphologies allowing for finer scale investigations of tissue-specific expression than can be conducted in *Corallorhiza*, due to a lack of leaf laminae and roots in the latter. However, the patterns of expression we inferred across *Corallorhiza* tissues are congruent with those known for *WHY1*. While gene-level expression inferred across tissues was highest for *C. wisteriana* and *C. trifida*, tissue-specific expression was only statistically significant in *C. trifida*, after correcting for repeated testing. Our inferences of *WHY1* expression among the belowground tissues of *Corallorhiza* provide for a hypothesized minimum expression level of canonical *WHY1*, which is similar to aboveground levels of expression in *Corallorhiza* species aside from *C. trifida*. Taken together, our results provide evidence for a trajectory beginning with differential expression of *WHY1* between aboveground and belowground tissues of the most photosynthetically capable *Corallorhiza* species to similar expression levels between above and belowground tissues of the latest stage mycoheterotrophic members of the genus. However, future work leveraging qPCR-derived estimates of *WHY1* expression across species and tissues is needed to corroborate the trends in expression patterns we characterize here. Taken together, our results suggest that alteration in expression or splicing of *WHY1* is unlikely to underlie the transition to mycoheterotrophy since the tissue-level

expression patterns of the gene in *C. trifida* are similar to those described from autotrophic plants.

Our work is the first to provide evidence for alternative splicing of, and intron retention in, *WHY1*. Approximately 70% of plant genes with multiple exons can be expected to be alternatively spliced (Reddy et al., 2013; Chamala et al., 2015), and intron retention is a common form of alternative splicing in plants (Ner-Gaon et al., 2004). Our finding of intron retention in one isoform from each *Corallorhiza* species aside from *C. trifida* is the first such event described for the gene. It has long been recognized that intron retention is most common in transcripts of genes like *WHY1* which serve roles related to photosynthesis and stress response (Ner-Gaon et al., 2004), a finding also supported by work investigating the effects of plant stressors on levels of alternative splicing (Filichkin et al., 2018; Jabre et al., 2019). In fact, tissue-specific differential intron retention has been shown to be an inducible stress response in *Populus trichocarpa* (Filichkin et al., 2018). Modification of *WHY1*, including inserted sequence, has long been used to study the effects of mutations on the function of the gene and to induce knockouts (Desveaux et al., 2004; Yoo et al., 2007; Maréchal et al., 2009), work which helped identify the many pathways that *WHY1* is involved in. For example, Yoo et al. (2007) and Maréchal et al. (2009) leveraged knockouts caused by T-DNA insertions into *WHY1* to reveal the critical role the gene plays in maintaining telomere length and plastome stability in *Arabidopsis thaliana*, respectively. Similarly, Prikryl et al. (2008) and Qiu et al. (2022) found that double knockout *WHY1* mutants were characterized by a lethal albino phenotype after the development of a few leaves, with Qiu et al. (2022) also characterizing divergent splicing and mRNA editing of plastid genes in *WHY1* mutants. The assembly of intron-retaining transcripts from all *Corallorhiza* species aside from *C. trifida*, and more transcriptional isoforms in *Corallorhiza* species in later stages of mycoheterotrophy, is suggestive of a negative correlation between increased splicing variation and both plastome stability and chlorophyll concentration in tissues (Barrett et al., 2014). However, future long-read sequencing of isoforms is needed to definitively verify assembled isoform variants and the presence of retained introns. We propose that it is unlikely that the intron-containing isoforms result in functional products, since a premature stop codon results from intron retention. The recovery of non-canonical and intron-retaining *WHY1* isoforms across individuals and tissues of *Corallorhiza* could be signal of idiosyncratic spliceosome regulation in mycoheterotrophic species, epitranscriptomic differences (Jabre et al., 2019), differential responses to stress in sampled tissues (Filichkin et al., 2018), or the expression of multiple, divergent copies of the gene. However, we hypothesize that reduced fidelity in the spliceosome of a mycoheterotrophic plant is the most likely cause of the observed splicing variation, given the phylogenetic and sequencing data at hand. We predict that changes in the expression and splicing of *WHY1* across *Corallorhiza* would likely be due to the alteration of one or more pathways involved in gene regulation, since we did find nucleotide-level changes that could be responsible.

Our work is the first to characterize the evolution of a transcription factor that could impact the genetic and phenotypic changes that occur along the path to full mycoheterotrophy. The previously characterized

roles that *WHY1* plays in plastome stability (Parent et al., 2011; Lepage et al., 2013), defense responses (Lin et al., 2020), and leaf senescence (Lin et al., 2019), together position the gene as a worthwhile target for the study of the molecular underpinnings of the transition to mycoheterotrophy. Heterotrophy in plants is associated with genomic restructuring, where a trend of plastome contraction and nuclear genome expansion via rampant repetitive element accumulation has commonly been observed (Barrett et al., 2014; Lyko and Wicke, 2021). Dramatic reductions of plastome length and gene content of mycoheterotrophic plants have been documented, ranging from minimal degradation in early transitional orchids such as *Corallorhiza* (Barrett and Davis, 2012) to pronounced degradation in late-transitional orchids such as *Epipogium* and *Pogoniopsis* (Schelkunov et al., 2015; Klimpert et al., 2022). Our finding of putatively functional *WHY1*, but the putative presence of increasingly alternatively spliced *WHY1* isoforms across the *Corallorhiza* trophic gradient is not necessarily surprising, given the minimally destabilized plastomes of the group. For example, Barrett and Davis (2012) found that the plastome of *C. striata*, the most destabilized of the *Corallorhiza* species included here, is only about 6% reduced relative to that of a leafy, autotrophic relative. Despite their relatively intact states, *Corallorhiza* plastomes are in various stages of degradation (Barrett et al., 2014), and our work here together suggests a negative correlation between both increased putatively aberrant splicing and nucleotide-level divergence of *WHY1* with plastome stability across the sampled species. Likewise, the plastomes of *Gastrodia elata* and *Epipogium aphyllum*, both late-stage mycoheterotrophs for which our analyses show that *WHY1* contains premature stop codons and significant signal of relaxed selection, are both extremely reduced and syntenically disrupted (Yuan et al., 2018; Chen et al., 2020; Xu et al., 2021). Taken together, our findings provide the first evidence of a potential negative correlation between increased divergence in sequence, splicing of *WHY1*, and plastome stability in early to late-stage mycoheterotrophic orchids.

5 Conclusions

Our work showcases the rich opportunities afforded by mycoheterotrophic plants not just for the study of the evolution of *WHY1* but for any gene of which homozygous knockouts can result in a fatal phenotype in autotrophic plants. Continued investigation of non-autotrophic plant lineages promises to fill gaps in our understanding of the precursors and consequences of genomic instability, and even the minimum gene space of land plants. Here we presented findings of non-synonymous nucleotide substitutions in functionally annotated regions in *Corallorhiza WHY1* sequence, and a high degree of divergence in *WHY1* in late-stage fully mycoheterotrophic orchids. However, our results together suggest that changes to the expression and splicing of *WHY1* may occur prior to the establishment of obviously deleterious genomic substitutions that would render the TF non-functional in late stage mycoheterotrophic orchids. In sum, our work characterizes *WHY1* variation and evolution throughout the angiosperms and serves as the first evidence of a potential correlation between decreased expression and increased

alternative splicing of *WHY1* concomitant with plastome degradation in a group of early transitional mycoheterotrophic orchids. However, our results do not implicate divergent *WHY1* function as a primary factor in the transition from partial to full mycoheterotrophy. Future work documenting differential non-canonical splicing and tissue-level expression of *WHY1 in vivo* are necessary to fully confirm the results of our transcriptomic analyses.

Data availability statement

The datasets presented in this study can be found in online repositories. The names of the repository/repositories and accession number(s) can be found below: Bioproject accession number: PRJNA984634.

Author contributions

BS and CB contributed to the conception and design of the study. CB collected *Corallorhiza* samples for RNA-seq. RM and BS collected all publicly available samples, conducted wet-lab work, Nanopore sequencing, and bioinformatic analyses. RM wrote the first manuscript draft. All authors contributed to the article and approved the submitted version.

Funding

Acknowledgments

Conflict of interest

The authors declare that the research was conducted in the absence of any commercial or financial relationships that could be construed as a potential conflict of interest.

Publisher's note

All claims expressed in this article are solely those of the authors and do not necessarily represent those of their affiliated organizations, or those of the publisher, the editors and the reviewers. Any product that may be evaluated in this article, or claim that may be made by its manufacturer, is not guaranteed or endorsed by the publisher.

Supplementary material

The Supplementary Material for this article can be found online at: https://www.frontiersin.org/articles/10.3389/fpls.2024.1241515/full#supplementary-material

References

Barrett, C. F., and Davis, J. I. (2012). The plastid genome of the mycoheterotrophic *Corallorhiza striata* (Orchidaceae) is in the relatively early stages of degradation. *Am. J. Bot.* 99, 1513–1523. doi: 10.3732/ajb.1200256

Barrett, C. F., and Freudenstein, J. V. (2008). Molecular evolution of *rbcL* in the mycoheterotrophic coralroot orchids (*Corallorhiza* Gagnebin, Orchidaceae). *Mol. Phylogenet. Evol.* 47, 665–679. doi: 10.1016/j.ympev.2008.02.014

Barrett, C. F., Freudenstein, J. V., Lee Taylor, D., and Kõljalg, U. (2010). Rangewide analysis of fungal associations in the fully mycoheterotrophic *Corallorhiza striata* complex (Orchidaceae) reveals extreme specificity on ectomycorrhizal *Tomentella* (Thelephoraceae) across North America. *Am. J. Bot.* 97, 628–643. doi: 10.3732/ajb.0900230

Barrett, C. F., Freudenstein, J. V., Li, J., Mayfield-Jones, D. R., Perez, L., Pires, J. C., et al. (2014). Investigating the path of plastid genome degradation in an early transitional clade of heterotrophic orchids, and implications for heterotrophic angiosperms. *Mol. Biol. Evol.* 31, 3095–3112. doi: 10.1093/molbev/msu252

Barrett, C. F., Pace, M. C., Corbett, C. W., Kennedy, A. H., Thixton-Nolan, H. L., and Freudenstein, J. V. (2024). Organellar phylogenomics at the epidendroid orchid base, with a focus on the mycoheterotrophic *Wullschlaegelia*. *Ann. Bot.* doi: 10.1093/aob/mcae084

Barrett, C. F., Sinn, B. T., and Kennedy, A. H. (2019). Unprecedented parallel photosynthetic losses in a heterotrophic orchid genus. *Mol. Biol. Evol.* 36, 1884–1902. doi: 10.1093/molbev/msz111

Barrett, C. F., Wicke, S., and Sass, C. (2018). Dense infraspecific sampling reveals rapid and independent trajectories of plastome degradation in a heterotrophic orchid complex. *New Phytol.* 218, 1192–1204. doi: 10.1111/nph.15072

Bolger, A. M., Lohse, M., and Usadel, B. (2014). Trimmomatic: a flexible trimmer for Illuminasequence data. *Bioinformatics* 30, 2114–2120. doi: 10.1093/bioinformatics/btu170

Bruce, B. D. (2001). The paradox of plastid transit peptides: conservation of function despitedivergence in primary structure. *Biochim. Biophys. Acta* 1541, 2–21. doi: 10.1016/S0167-4889(01)00149-5

Bushnell, B. B. (2022) *bbtools*. Available online at: https://sourceforge.net/projects/bbmap/files.

Cai, L. (2023). Rethinking convergence in plant parasitism through the lens of molecular and population genetic processes. *Am. J. Bot.* 110 (5), e16174. doi: 10.1002/ajb2.16174

Cai, J., Liu, X., Vanneste, K., Proost, S., Tsai, W.-C., Liu, K.-W., et al. (2015). The genome sequence of the orchid *Phalaenopsis equestris*. *Nat. Genet.* 47, 65–72. doi: 10.1038/ng.3149

Cameron, D. D., Preiss, K., Gebauer, G., and Read, D. J. (2009). The chlorophyll-containingorchid *Corallorhiza trifida* derives little carbon through photosynthesis. *New Phytol.* 183, 358–364. doi: 10.1111/j.1469-8137.2009.02853.x

Cappadocia, L., Maréchal, A., Parent, J.-S., and Lepage, É. (2010). Crystal structures of DNA Whirly complexes and their role in *Arabidopsis* organelle genome repair. *Plant Cell* 22, 1849–1867. doi: 10.1105/tpc.109.071399

Cappadocia, L., Parent, J.-S., Sygusch, J., and Brisson, N. (2013). A family portrait: structural comparison of the Whirly proteins from *Arabidopsis thaliana* and *Solanum tuberosum*. *Acta Crystallographica Section* F69, 1207–1211. doi: 10.1107% 2FS1744309113028698

Chamala, S., Feng, G., Chavarro, C., and Barbazuk, W. B. (2015). Genome-wide identification of evolutionarily conserved alternative splicing events in flowering plants. *Front. Bioengineering Biotechnol.* 3, 33. doi: 10.3389/fbioe.2015.00033

Chao, Y.-T., Yen, S.-H., Yeh, J.-H., Chen, W.-C., and Shih, M.-C. (2017). Orchidstra 2.0 – a transcriptomics resource for the orchid family. *Plant Cell Physiol.* 58, e9. doi: 10.1093/pcp/pcw220

Chen, Y.-Y., Li, C.-I., Hsiao, Y.-Y., Ho, S.-Y., Zhang, Z.-B., Liao, C.-C., et al. (2022). OrchidBase 5.0: updates of the orchid genome knowledgebase. *BMC Plant Biol.* 22, 557. doi: 10.1186/s12870-022-03955-5

Chen, S., Wang, X., Wang, Y., Zhang, G., Song, W., Dong, X., et al. (2020). Improved *de novo* assembly of the achlorophyllous orchid *Gastrodia elata*. *Front. Genet.* 11, 580568. doi: 10.3389/fgene.2020.580568

Chernomor, O., von Haeseler, A., and Minh, B. Q. (2016). Terrace aware data structure for phylogenomic inference from supermatrices. *Systematic Biol.* 65, 997–1008. doi: 10.1093/sysbio/syw037

Christian, R. W., Hewitt, S. L., Nelson, G., Roalson, E. H., and Dhingra, A. (2020). Plastid transit peptides—where do they come from and where do they all belong? Multi-genome and pan-genomic assessment of chloroplast transit peptide evolution. *PeerJ* 8, e9772. doi: 10.7717/peerj.9772

de Mendoza, A., Sebé-Pedrós, A., Ŝestak, M. S., Matejčić, M., Torruella, G., Domazet-Lošo, T., et al. (2013). Transcription factor evolution in eukaryotes and the assembly of the regulatory toolkit in multicellular lineages. *Proc. Natl. Acad. Sci. United States America* 110, E4858–E4866. doi: 10.1073/pnas.1311818110

De Smet, R., Adams, K. L., Vandepoele, K., Van Montagu, M. C. E., Maere, S., and Van de Peer, Y. (2013). Convergent gene loss following gene and genome duplications creates single-copy families in flowering plants. *Proc. Acad. Sci. United States America* 110, 2898–2903. doi: 10.1073/pnas.1300127110

Desveaux, D., Allard, J., Brisson, N., and Sygusch, J. (2002). A new family of plant transcriptionfactors displays a novel ssDNA-binding surface. *Nat. Struct. Mol. Biol.* 9, 512–517. doi: 10.1038/nsb814

Desveaux, D., Després, C., Joyeux, A., Subramaniam, R., and Brisson, N. (2000). PBF-2 is a novel single-stranded DNA binding factor implicated in *PR-10a* gene activation in potato. *Plant Cell* 12, 1477–1489. doi: 10.1105/tpc.12.8.1477

Desveaux, D., Maréchal, A., and Brisson, N. (2005). Whirly transcription favors: defense gene regulation and beyond. *Trends Plant Sci.* 10, 1360–1385. doi: 10.1016/j.tplants.2004.12.008

Desveaux, D., Subramaniam, R., Després, C., Mess, J.-N., Lévesque, C., Fobert, P. R., et al. (2004). A "whirly" transcription factor is required for salicylic acid dependent disease resistance in *Arabidopsis*. *Dev. Cell* 6, 229–240. doi: 10.1016/S1534-5807(04)00028-0

Doyle, J. J., Davis, J. I., Soreng, R. J., Garvin, D., and Anderson, M. J. (1992). Chloroplast DNA inversions and the origin of the grass family. *Proc. Natl. Acad. Sci. United States America* 89, 7722–7726. doi: 10.1073%2Fpnas.89.16.7722

Doyle, J. J., and Doyle, J. L. (1987). A rapid DNA isolation procedure for small quantities of fresh leaf tissue. *Phytochemical Bull.* 19, 11–15.

Duarte, J. M., Wall, P. K., Edger, P. P., Landherr, L. L., Ma, H., Pires, J. C., et al. (2010). Identification of shared single copy nuclear genes in Arabidopsis, Populus, *Vitis* and *Oryza* and their phylogenetic utility across various taxonomic levels. *BMC Evolutionary Biol.* 10, 61. doi: 10.1186/1471-2148-10-61

Eddy, S. R. (2011). Accelerated profile HMM searches. *PloS Comput. Biol.* 7, e1002195. doi: 10.1371/journal.pcbi.1002195

Emms, D. M., and Kelly, S. (2015). OrthoFinder: solving fundamental biases in whole genome comparisons dramatically improves orthogroup inference accuracy. *Genome Biol.* 16, 157. doi: 10.1186/s13059-015-0721-2

Emms, D. M., and Kelly, S. (2019). OrthoFinder: phylogenetic orthology inference for comparative genomics. *Genome Biol.* 20, 238. doi: 10.1186/s13059-019-1832-y

Felsenstein, J. (1985). Phylogenies and the comparative method. *Am. Nat.* 125, 1–15. doi: 10.1086/284325

Filichkin, S. A., Hamilton, M., Dharmawardhana, P. D., Singh, S. K., Sullivan, C., Ben-Hur, A., et al. (2018). Abiotic stresses modulate landscape of *Popular* transcriptome via alternative splicing, differential intron retention, and isoform ratio switching. *Front. Plant Sci.* 9, 5. doi: 10.3389/fpls.2018.00005

Foyer, C. H., Karpinska, B., and Krupinska, K. (2014). The functions of WHIRLY1 and REDOXRESPONSIVE TRANSCRIPTION FACTOR 1 in cross tolerance

responses in plants: a hypothesis. *Philos. Trans. R. Soc. B* 369, 20130226. doi: 10.1098%2Frstb.2013.0226

Freudenstein, J. V., and Barrett, C. F. (2014). Fungal host utilization helps circumscribe leafless Coralroot orchid species: an integrative analysis of Corallorhiza odontorhiza and C. wisteriana. *Taxon* 63 (4), 759–772. doi: 10.12705/634.3

Givnish, T. J., Spali nk, D., Ames, M., Lyon, S. P., Hunter, S. J., Zuluaga, A., et al. (2016). Orchid historical biogeography, diversification, Antarctica and the paradox of orchid dispersal. *J. Biogeography* 43, 1905–1916. doi: 10.1111/jbi.12854

Grabherr, M. G., Haas, B. J., Yassour, M., Levin, J. Z., Thompson, D. A., Amit, I., et al. (2011). Full-length transcriptome assembly from RNA-Seq data without a reference genome. *Nat. Biotechnol.* 29, 644–652. doi: 10.1038/nbt.1883

Grabowski, E., Miao, Y., Mulisch, M., and Krupinska, K. (2008). Single-stranded DNA-binding protein Whirly1 in barley leaves is located in plastids and the nucleus of the same cell. *Plant Physiol.* 147, 1800–1804. doi: 10.1104/pp.108.122796

Graham, S. W., Lam, V. K. Y., and Merckx, V. S. F. T. (2017). Plastomes on the edge: the evolutionary breakdown of mycoheterotroph plastid genomes. *New Phytol.* 214, 48–55. doi: 10.1111/nph.14398

Guo, X., Fang, D., Sahu, S. K., Yang, S., Guang, X., Folk, R., et al. (2021). *Chloranthus* genome provides insights into the early diversification of angiosperms. *Nat. Commun.* 12, 6930. doi: 10.1038/s41467-021-26922-4

Haas, B. J., Papanicolaou, A., Yassour, M., Grabherr, M., Blood, P. D., Bowden, J., et al. (2013). *De novo* transcript sequence reconstruction from RNA-seq using the Trinity platform for reference generation and analysis. *Nat. Protoc.* 8, 1494–1512. doi: 10.1038/nprot.2013.084

Hoang, D. T., Chernomor, O., von Haeseler, A., Minh, B. Q., and Vinh, L. S. (2018). UFBoot2: improving the ultrafast bootstrap approximation. *Mol. Biol. Evol.* 35, 518–522. doi: 10.1093/molbev/msx281

Isemer, R., Mulisch, M., Schäfer, A., Kirchner, S., Koop, H.-U., and Krupinksa, K. (2012). Recombinant Whirly1 translocates from transplastomic chloroplasts to the nucleus. *Fed. Eur. Biochem. Societies Lett.* 586, 85–88. doi: 10.1016/j.febslet.2011.11.029

Jabre, I., Reddy, A. S. N., Kalyna, M., Chaudhary, S., Khokhar, W., Byrne, L. J., et al. (2019). Does co-transcriptional regulation of alternative splicing mediate plant stress responses? *Nucleic Acids Res.* 47, 2716–2726. doi: 10.1093/nar/gkz121

Kalyaanamoorthy, S., Minh, B. Q., Wong, T. K. F., von Haeseler, A., and Jermiin, L. S. (2017). ModelFinder: fast model selection for accurate phylogenetic estimates. *Nat. Methods* 14, 587–589. doi: 10.1038/nmeth.4285

Katoh, K., Misawa, K., Kuma, K., and Miyata, T. (2002). MAFFT: a novel method for rapid multiple sequence alignment based on fast Fourier transform. *Nucleic Acids Res.* 30, 3059–3066. doi: 10.1093/nar/gkf436

Katoh, K., and Standley, D. M. (2013). MAFFT multiple sequence alignment software version 7: improvements in performance and usability. *Mol. Biol. Evol.* 30, 772–780. doi: 10.1093/molbev/mst010

Klepikova, A. V., Kasianov, A. S., Gerasimov, E. S., Logacheva, M. D., and Penin, A. A. (2016). A high resolution map of the *Arabidopsis thaliana* developmental transcriptome based on RNA-seq profiling. *Plant J.* 88, 1058–1070. doi: 10.1111/tpj.13312

Klimpert, N. J., Mayer, J. L. S., Sarzi, D. S., Prosdocimi, F., Pinheiro, F., and Graham, S. W. (2022). Phylogenomics and plastome evolution of a Brazilian mycoheterotrophic orchid, *Pogoniopsis schenckii*. *Am. J. Bot.* 109, 2030–2050. doi: 10.1002/ajb2.16084

Krause, K., Kilbienski, I., Mulisch, M., Rödiger, A., Schäfer, A., and Krupinksa, K. (2005). DNA-binding proteins of the Whirly family in *Arabidopsis thaliana* are targeted to the organelles. *Fed. Eur. Biochem. Societies Lett.* 579, 3707–3712. doi: 10.1016/j.febslet.2005.05.059

Lai, X., Chahtane, H., Martin-Arevalillo, R., Zubita, C., and Parcy, F. (2020). Contrasted evolutionary trajectories of plant transcription factors. *Curr. Opin. Plant Biol.* 54, 101–107. doi: 10.1016/j.pbi.2020.03.002

Lallemand, F., Martin-Magniette, M., Gilard, F., Gakière, B., Launay-Avon, A., Delannoy, É., et al. (2019). *In situ* transcriptomic and metabolomic study of the loss of photosynthesis in the leaves of mixotrophic plants exploiting fungi. *Plant J.* 98, 826–841. doi: 10.1111/tpj.14276

Latchman, D. S. (1993). Transcription factors: an overview. *Int. J. Exp. Pathol.* 74, 417–422.

Leake, J. R. (1994). The biology of myco-heterotrophic ("saprophytic") plants. *New Phytol.* 127, 171–216. doi: 10.1111/j.1469-8137.1994.tb04272.x

Lee, C., Ruhlman, T., and Jansen, R. K. (2020). Unprecedented intraindividual structural heteroplasmy in *Eleocharis* (Cyperaceae, Poales) Plastomes. *Genome Biol. Evol.* 12, 641–655. doi: 10.1093/gbe/evaa076

Lehti-Shiu, M. D., Panchy, N., Wang, P., Uygun, S., and Shiu, S.-H. (2017). Diversity, expansion, and evolutionary novelty of plant DNA-binding transcription factor families. *Biochim. Biophys. Acta* 1860, 3–20. doi: 10.1016/j.bbagrm.2016.08.005

Lemaire, B., Huysmans, S., Smets, E., and Merckx, V. S. F. T. (2010). Rate accelerations in nuclear 18S rDNA of mycoheterotrophic and parasitic angiosperms. *J. Plant Res.* 124, 561–576. doi: 10.1007/s10265-010-0395-5

Lepage, É., Zampini, É., and Brisson, N. (2013). Plastid genome instability leads to reactive oxygen species production and plastid-to-nucleus retrograde signaling in *Arabidopsis*. *Plant Physiol.* 163, 867–881. doi: 10.1104/pp.113.223560

Li, H. (2018). Minimap2: pairwise alignment for nucleotide sequences. *Bioinformatics* 34, 3094–3100. doi: 10.1093/bioinformatics/bty191

Li, H., Handsaker, B., Wysoker, A., Fennell, T., Ruan, J., Homer, N., et al. (2009). The sequence alignment/map (SAM) format and SAMtools. *Bioinformatics* 25, 2078–2079. doi: 10.1093/bioinformatics/btp352

Li, Y. X., Li, Z. H., Schuiteman, A., Chase, M. W., Li, J.-W., Huang, W. C., et al. (2019). Phylogenomics of Orchidaceae based on plastid and mitochondrial genomes. *Mol. Phylogenet. Evol.* 139, 106540. doi: 10.1016/j.ympev.2019.106540

Lin, W., Huang, D., Shi, X., Deng, B., Ren, Y., Lin, W., et al. (2019). H_2O_2 as a feedback signal on dual-located WHIRLY1 associates with leaf senescence in *Arabidopsis*. *Cells* 8 (12), 1585. doi: 10.3390/cells8121585

Lin, W., Zhang, H., Huang, D., Schenke, D., Cai, D., Wu, B., et al. (2020). Dual-localized WHIRLY1 affects alicyclic acid biosynthesis via coordination of ISOCHORISMATE SYNTHASE1, PHENYLALANINE AMMONIA LYASE1, and S-ADENOSYL-L-METHIONINE-DEPENDENT METHYLTRANSFERASE1. *Plant Physiol.* 1840, 1884–1899. doi: 10.1104/pp.20.00964

Liu,, Jung, J. C., Xu, J., Wang, H., Deng, S., Bernad, L., et al. (2012). Genome-wide analysis uncovers regulation of long intergenic noncoding RNAs in *Arabidopsis*. *Plant Cell* 24, 4333–4345. doi: 10.1105/tpc.112.102855

Lyko, P., and Wicke, S. (2021). Genomic reconfiguration in parasitic plants involves considerable gene losses alongside global genome size inflation and gene births. *Plant Physiol.* 186, 1412–1423. doi: 10.1093/plphys/kiab192

Maddison, W. P. (1997). Gene trees in species trees. *Systematic Biol.* 46, 523–536. doi: 10.1093/sysbio/46.3.523

Maréchal, A., Parent, J. S., Véronneau-Lafortune, F., Joyeux, A., Lang, B. F., and Brisson, N. (2009). Whirly proteins maintain plastid genome stability in Arabidopsis. *Proc. Natl. Acad. Sci. United States America* 106, 14693–14698. doi: 10.1073/pnas.0901710106

Merckx, V. S. F. T., and Freudenstein, J. V. (2010). Evolution of mycoheterotrophy in plants: a phylogenetic perspective. *New Phytol.* 185, 605–609. doi: 10.1111/j.1469-8137.2009.03155.x

Merckx, V. S. F. T., and Merckx, V. S. F. T. (2013). "Mycoheterotrophy: an introduction," in *Mycoheterotrophy: the biology of plants living on fungi, 1st ed* (Springer, NY). doi: 10.1007/978-1-4614-5209-6

Mergner, J., Fresno, M., List, M., Papacek, M., Chen, X., Chaudhary, A., et al. (2020). Mass-spectrometry-based draft of the *Arabidopsis* proteome. *Nature* 579, 409–414. doi: 10.1038/s41586-020-2094-2

Münster, T., Pahnke, J., Di Rosa, A., Kim, J. T., Martin, W., Saedler, H., et al. (1997). Floral homeotic genes were recruited from homologous MADS-box genes preexisting in the common ancestor of ferns and seed plants. *Proc. Natl. Acad. United States America* 94, 3415–2420. doi: 10.1073%2Fpnas.94.6.2415

Murrell, B, Moola, S., Mabona, A., Weighill, T., Sheward, D., Pond, S. L. K., et al. (2013). FUBAR: A Fast, Unconstrained Bayesian AppRoximation for inferring selection. *Mol. Biol. Evol.* 30), 1196–1205. doi: 10.1093/molbev/mst030

Murrell, B., Weaver, S., Smith, M. D., Wertheim, J. O., Murrell, S., Aylward, A., et al. (2015). Gene-wide identification of episodic selection. *Mol. Biol. Evol.* 32, 1365–1371. doi: 10.1093/molbev/msv035

Ner-Gaon, H., Halachmi, R., Savaldi-Goldstein, S., Rubin, E., Ophir, R., and Fluhr, R. (2004). Intronretention is a major phenomenon in alternative splicing in *Arabidopsis*. *Plant J.* 39, 877–885. doi: 10.1111/j.1365-313x.2004.02172.x

Nguyen, L.-T., Schmidt, H. A., von Haeseler, A., and Minh, B. Q. (2015). IQ-TREE: A fast and effective stochastic algorithm for estimating maximum-likelihood phylogenies. *Mol. Biol. Evol.* 32, 268–274. doi: 10.1093/molbev/msu300

Pamilo, P., and Nei, M. (1988). Relationships between gene trees and species trees. *Mol. Biol. Evol.* 5, 568–583. doi: 10.1093/oxfordjournals.molbev.a040517

Parent, J.-S., Lepage, E., and Brisson, N. (2011). Divergent roles for the two polI-like organelle DNA polymerases of *Arabidopsis*. *Plant Physiol.* 156, 254–262. doi: 10.1104/pp.111.173849

Patro, R., Duggal, G., Love, M. I., Irizarry, R. A., and Kingsford, C. (2017). Salmon provides fast and bias-aware quantification of transcript expression. *Nat. Methods* 14, 417–419. doi: 10.1038/nmeth.4197

Patron, N. J., and Waller, R. F. (2007). Transit peptide diversity and divergence: a global analysis of plastid targeting signals. *BioEssays* 29, 1048–1058. doi: 10.1002/bies.20638

Pérez-Escobar, O. A., Bogarín, D., Przelomska, N. A. S., Ackerman, J. D., Balbuena, J. A., Bellot, S., et al. (2024). The origin and speciation of orchids. *New Phytol.* 242, 700–716. doi: 10.1111/nph.19580

Pérez-Escobar, O. A., Dodsworth, S., Bogarín, D., Bellot, S., Balbuena, J. A., Schely, R. J., et al. (2021). Hundreds of nuclear and plastid loci yield novel insights into orchid relationships. *Am. J. Bot.* 108, 1166–1180. doi: 10.1002/ajb2.1702

Pond, S. L. K., and Muse, S. V. (2005). "HyPhy: hypothesis testing using phylogenies," in *Statistical methods in molecular evolution, 1st ed*. Ed. R. Nielsen (Springer, NY).

Pond, S. L. K., Posada, D., Gravenor, M. B., Woelk, C. H., and Frost, S. D. W. (2006). GARD: a genetic algorithm for recombination detection. *Bioinformatics* 22, 3096–3098. doi: 10.1093/bioinformatics/btl474

Prikryl, J., Watkins, K. P., Friso, G., van Wijk, K. J., and Barkan, A. (2008). A member of the Whirly family is a multifunctional RNA- and DNA-binding protein that is

essential for chloroplast biogenesis. *Nucleic Acids Res.* 36, 5152–5165. doi: 10.1093/nar/gkn492

Qiu, Z., Chen, D., Teng, L., Guan., P., Yu, G., Zhang, P., et al. (2022). OsWHY1 interacts with OsTRXz and is essential for early chloroplast development in rice. *Rice* 15, 50. doi: 10.1186/s12284-022-00596-y

Ranwez, V., Harispe, S., Delsuc, F., and Douzery, E. J. P. (2011). MACSE: multiple alignment ofcoding sequences accounting for frameshifts and stop codons. *PloS One* 6, e22594. doi: 10.1371/journal.pone.0022594

Rasmussen, H. N. (1995). *Terrestrial orchids: from seed to mycotrophic plant* (Cambridge: Cambridge University Press). doi: 10.1017/CBO9780511525452

Rasmussen, H. N. (2002). Recent developments in the study of orchid mycorrhiza. *Plant Soil* 244, 149–163. doi: 10.1023/A:1020246715436

R Core Team (2019). *R: A language and environment for statistical computing* (Vienna, Austria: The R Foundation). Available at: https://www.R-project.org/.

Reddy, A. S., Marquez, Y., Kalyna, M., and Barta, A. (2013). Complexity of the alternative splicing landscape in plants. *Plant Cell* 25, 3657–3683. doi: 10.1105/tpc.113.117523

Ren, Y., Li, Y., Jiang, Y., Wu, B., and Miao, Y. (2017). Phosphorylation of WHIRLY1 by CIPK14 shifts its localization and dual functions in *Arabidopsis*. *Mol. Plant* 10, 749–763. doi: 10.1016/j.molp.2017.03.011

Robinson, M. D., McCarthy, D. J., and Smyth, G. K. (2010). edgeR: a Bioconductor package for differential expression analysis of digital gene expression data. *Bioinformatics* 26, 139–140. doi: 10.1093/bioinformatics/btp616

Robinson, M. D., and Oshlack, A. (2010). A scaling normalization method for differential expression analysis of RNA-seq data. *Genome Biol.* 11, R25. doi: 10.1186/gb-2010-11-3-r25

Ruan, Q., Wang, Y., Xu, H., Wang, B., Zhu, X., Wei, B., et al. (2022). Genome-wide identification, phylogenetic, and expression analysis under abiotic stress conditions of Whirly (WHY) gene family in *Medicago sativa* L. *Sci. Rep.* 12, 18676. doi: 10.1038/s41598-022-22658-3

Schelkunov, M. I., Shtratnikova, V. Y., Nuraliev, M. S., Selosse, M.-A., Penin, A. A., and D.Logacheva, M. (2015). Exploring the limits for reduction of plastid genomes: a case study of the mycoheterotrophic orchids *Epipogium aphyllum* and *Epipogium roseum*. *Genome Biol. Evol.* 7, 1179–1191. doi: 10.1093/gbe/evv019

Serna-Sánchez, M. A., Pérez-Escobar, O. A., Bogarín, D., Torres-Jimenez, F. F., Alvarez-Yela, A. C., Arcila-Galvis, J. E., et al. (2021). Plastid phylogenomics resolves ambiguous relationships within the orchid family and provides a solid timeframe for biogeography and macroevolution. *Sci. Rep.* 11, 6858. doi: 10.1038/s41598-021-83664-5

Sinn, B. T., and Barrett, C. F. (2020). Ancient mitochondrial gene transfer between fungi and theorchids. *Mol. Biol. Evol.* 37, 44–57. doi: 10.1093/molbev/msz198

Suetsugu, K., Yamato, M., Miura, C., Yamaguchi, K., Takahashi, K., Ida, Y., et al. (2017). Comparison of green and albino individuals of the partially mycoheterotrophic orchid *Epipactis helleborine* on molecular identities of mycorrhizal fungi, nutritional modes and gene expression in mycorrhizal roots. *Mol. Ecol.* 26, 1652–1669. doi: 10.1111/mec.14021

Sun, S., Li, S., Zhou, X., and Yang, X. (2023). WRKY1 represses the WHIRLY1 transcription factor to positively regulate plant defense against geminivirus infection. *PloS Pathog.* 19, e1011319. doi: 10.1371/journal.ppat.1011319

Taylor, D. L., and Bruns, T. D. (1997). Independent, specialized invasions of ectomycorrhizal mutualism by two nonphotosynthetic orchids. *Proc. Natl. Acad. United States America*. 94, 4510–4515. doi: 10.1073/pnas.94.9.4510

Taylor, R. E., West, C. E., and Foyer, C. H. (2022). WHIRLY protein functions in plants. *Food Energy Secur.* 00, e379. doi: 10.1002/fes3.379

The Angiosperm Phylogeny Group, Chase, M. W., Christenhusz, M. J. M., Fay, M. F., Byng, J. W., Judd, W. S., et al. (2016). An update of the Angiosperm Phylogeny Classification for the orders and families of flowering plants: APG IV. *Botanical J. Linn. Society.* 181, 1–20. doi: 10.1111/boj.12385

The Potato Genome Sequencing Consortium (2011). Genome sequence and analysis of the tuber crop potato. *Nature* 475, 189–195. doi: 10.1038/nature10158

Timilsena, P. R., Barrett, C. F., Piñeyro-Nelson, A., Wafula, E. K., Ayyampalayam, S., McNeal, J. R., et al. (2023). Phylotranscriptomic analyses of mycoheterotrophic monocots show a continuum of convergent evolutionary changes in expressed nuclear genes from three independent nonphotosynthetic lineages. *Genome Biol. Evol.* 15, evac183. doi: 10.1093/gbe/evac183

Untergasser, A., Cutcutache, I., Koressaar, T., Ye, J., Faircloth, B. C., Remm, M., et al. (2012). Primer3-new capabilities and interfaces. *Nucleic Acids Res.* 40, e115. doi: 10.1093/nar/gks596

Waterworth, W. M., Drury, G. E., Bray, C. M., and West, C. E. (2011). Repairing breaks in the plant genome: the importance of keeping it together. *New Phytol.* 192, 805–822. doi: 10.1111/j.1469-8137.2011.03926.x

Wertheim, J. O., Murrell, B., Smith, M. D., Pond, S. L. K., and Scheffler, K. (2015). RELAX:detecting relaxed selection in a phylogenetic framework. *Mol. Biol. Evol.* 32), 820–832. doi: 10.1093/molbev/msu400

Wheeler, T. J., and Eddy, S. R. (2013). nhmmer: DNA homology search with profile HMMs. *Bioinformatics* 29 (19), 2487–2489. doi: 10.1093/bioinformatics/btt403

Wicke, S., Müller, K. F., dePamphilis, C. W., Quandt, D., Bellot, S., and Schneeweiss, G. M. (2016). Mechanistic model of evolutionary rate variation en route to a

nonphotosynthetic lifestyle in plants. *Proc. Natl. Acad. Sci. United States America* 113, 9045–9050. doi: 10.1073/pnas.1607576113

Wu,, Mueller, F. L. A., Crouzillat, D., Pétiard, V., and Tanksley, S. D. (2006). Combining bioinformatics and phylogenetics to identify large sets of single-copy orthologous genes (COSII) for comparative, evolutionary, and systematic studies: a test case in the euasterid plant clade. *Genetics* 174, 1407–1420. doi: 10.1534/genetics.106.062455

Xu, Y., Lei, Y., Su, Z., Zhao, M., Zhang, J., Shen, G., et al. (2021). A chromosome-scale *Gastrodia elata* genome and large-scale comparative genomic analysis indicate convergent evolution by gene loss in mycoheterotrophic and parasitic plants. *Plant J.* 108, 1609–1623. doi: 10.1111/tpj.15528

Yoo, H. H., Kwon, C., Lee, M. M., and Chung, I. K. (2007). Single-stranded DNA binding factor AtWHY1 modulates telomere length homeostasis in *Arabidopsis*. *Plant J.* 49, 442–451. doi: 10.1111/j.1365-313X.2006.02974.x

Yuan, Y., Jin, X., Liu, J., Zhao, X., Zhou, J., Wang, X., et al. (2018). The *Gastrodia elata* genome provides insights into plant adaptation to heterotrophy. *Nat. Commun.* 9, 1615. doi: 10.1038/s41467-018-03423-5

Zampini, É., Lepage, É., Tremblay-Belzile, S., Truche, S., and Brisson, N. (2015). Organelle DNA rearrangement mapping reveals U-turn-like inversions as a major source of genomic instability in *Arabidopsis* and humans. *Genome Res.* 25, 645–654. doi: 10.1101/gr.188573.114

Zeng, X., Li, Y., Ling, H., Liu, S., Liu, M., Chen, J., et al. (2017). Transcriptomic analyses reveal clathrin-mediated endocytosis involved in symbiotic seed germination of *Gastrodia elata*. *Botanical Stud.* 58, 31. doi: 10.1186/s40529-017-0185-7

Zhang, G., Hu, Y., Huang, M.-Z., Huang, W.-C., Liu, D.-K., Zhang, D., et al. (2023). Comprehensive phylogenetic analyses of Orchidaceae using nuclear genes and evolutionary insights into epiphytism. *J. Integr. Plant Biol.* 65, 1204–1225. doi: 10.1111/jipb.13462

Zhang, G.-Q., Liu, K.-W., Lohaus, R., Hsiao, Y.-Y., Niu, S.-C., Wang, J.-Y., et al. (2017). The *Apostasia* genome and the evolution of orchids. *Nature* 549 (7672), 379–383. doi: 10.1038/nature23897

Zhang, G.-Q., Xu, Q., Bian, C., Tsai, W.-C., Yeh, C.-M., Liu, K.-W., et al. (2016). The *Dendrobium catenatum* Lindl. genome sequence provides insights into polysaccharide synthase, floral development and adaptive evolution. *Sci. Rep.* 6, 19029. doi: 10.1038/srep19029

Zhao, S. Y., Wang, G. D., Zhao, W. Y., Zhang, S., Kong, F. Y., Dong, X. C., et al. (2018). Overexpression of tomato WHIRLY protein enhances tolerance to drought stress and resistance to *Pseudomonas solanacearum* in transgenic tobacco. *Biol. Plantarum* 62, 55–68. doi: 10.1007/s10535-017-0714-y

Zhao, T., Zwaenepoel, A., Xue, J.-Y., Kao, S.-M., Li, Z., Schranz, M. E., et al. (2021). Whole-genome microsynteny-based phylogeny of angiosperms. *Nat. Commun.* 12, 3498. doi: 10.1038/s41467-021-23665-0

Zhuang, K., Kong, F., Zhang, S., Meng, C., Yang, M., Liu, Z., et al. (2019). Whirly1 enhances tolerance to chilling stress in tomato via protection of photosystem II and regulation of starch degradation. *New Phytol.* 221, 1998–2012. doi: 10.1111/nph.15532

Zhuang, K., Wang, J., Jiao, B., Chen, C., Zhang, J., Ma, N., et al. (2020). WHIRLY1 maintains leaf photosynthetic capacity in tomato by regulating the expression of *RbcS1* under chilling stress. *J. Exp. Bot.* 12, 3653–3663. doi: 10.1093/jxb/eraa145

Zimmer, K., Meyer, C., and Gebauer, G. (2008). The ectomycorrhizal specialist orchidCorallorhiza trifida is a partial myco-heterotroph. *New Phytol.* 178, 395–400. doi: 10.1111/j.1469-8137.2007.02362.x